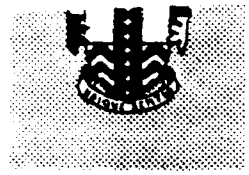

RSRE MEMORANDUM No. 4502

ROYAL SIGNALS & RADAR ESTABLISHMENT

ELECTROMAGNETIC SCATTERING BY THE DELTA BOUNDARY OPERATOR METHOD

Author: I D King

PROCUREMENT EXECUTIVE,
MINISTRY OF DEFENCE,
RSRE MALVERN,
WORCS.

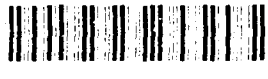

UNLIMITED

RSRE MEMORANDUM No. 4502

CONDITIONS OF RELEASE

0105887 303456

********** DRIC U

********** DRIC Y

Reports quoted are not necessarily available to members of the public or to commercial organisations.

DEFENCE RESEARCH AGENCY, ELECTRONICS DIVISION

MEMORANDUM No. 4502

Electromagnetic Scattering by the Delta Boundary Operator Method

I.D.King
AD2 Division
DRA Electronics Division
RSRE Malvern
St.Andrews Road
Malvern
Worcestershire WR14 3PS

July 1991

Abstract

An alternative and rigorous formulation of electromagnetic scattering — the Delta Boundary Operator (DBO) technique — has been reported in the literature. Use of a simple approximation allows fast and accurate calculations of scattering by rough planar surfaces. Here an investigation of the wider applicability of approximate DBO techniques is pursued. Attention is focussed on scattering by simple smooth bodies in the so-called resonance region, where the approximations of high frequency asymptotic techniques are often inadequate. It is shown that application of approximate DBO methods leads to predictions of non-vanishing surface currents in unlit regions and smooth transition currents at shadow boundaries.

INTENTIONALLY BLANK

Contents

1 Introduction 1

2 Principles of the Rigorous DBO Technique 2
- 2.1 Scattering by an infinite perfectly conducting plane 4
- 2.2 Scattering by a perfectly conducting circular cylinder 5

3 Principles of the Approximate DBO (ADBO) Technique 7

4 Application of ADBO Theory to Scattering by a Circular Cylinder 10

5 Analysis of the ψ-Distribution of the Circular Cylinder 14

6 Application of IDBO Theory to Scattering by a Circular Cylinder 18

7 Prescription of the IDBO Technique for a General Two-Dimensional Smooth Scatterer 21

8 Conclusions and Suggestions for Further Work 23

9 References 25

A Analysis of the Integral $I_\pi(\theta, ka)$ 27
- A.1 Stationary Phase Point Contributions 28
- A.2 End-Point Contributions 30

B Asymptotic ($ka \gg 1$) Analysis of $\psi^c(s, 0)$ 33

C Analysis of the Integral $M_\pi(\theta, ka)$ 37
- C.1 Saddle Point Contributions 37
- C.2 End-Point Contributions 38

D Contribution of $\psi^{c(2)}(s, 0)$ to the Cylinder Current 39

INTENTIONALLY BLANK

1 Introduction

Electromagnetic scattering by bodies up to a few wavelengths in size can be calculated using wire grid or surface patch modelling in conjunction with the method of moments. High frequency techniques such as the Geometrical Theory of Diffraction (GTD) or Physical Optics (PO) supplemented by a form of the Physical Theory of Diffraction (PTD) can often be successfully applied to larger objects. However with complex scatterers there is often an intermediate region where the computational requirements of moment method calculations are too great and where the approximations of the high frequency asymptotic techniques are inadequate. Scattering by bodies of this size is a topic currently attracting a great deal of interest.

An alternative and rigorous formulation of electromagnetic scattering - called the Delta Boundary Operator (DBO) technique - has been reported by Maystre [1] and by Saillard, Roger and Maystre [2]. Central to this scheme is the solution of an abstract boundary value problem from which the solution of a physical scattering problem can be derived. It has been shown [3,4] that a simple approximation to the solution of the intermediate problem allows fast and accurate calculations of scattering by rough planar surfaces where the scale of the roughness is of the order of the wavelength of the incident radiation. In particular the solutions are more accurate than those obtained by using Beckmann's method [5,6], a high frequency technique which uses the Kirchoff approximation. In this paper an investigation of the wider applicability of approximate DBO techniques is pursued. Attention is focussed on scattering by simple smooth bodies. Emphasis is given to scattering by objects in the resonance region and comparison is made with the PO technique.

In Section 2 the principles of the rigorous DBO formulation are outlined and illustrated with simple examples. A simple approximate DBO (ΛDBO) theory is developed in Section 3 and this is applied to plane wave scattering by a conducting circular cylinder in Section 4. Some refinement is seen to be necessary for accurate current and radar cross section (RCS) predictions and an improved DBO (IDBO) procedure is proposed in Section 5. This is tested by application to the circular cylinder problem in Section 6 and is prescribed for a general smooth two-dimensional ($2D$) scatterer in Section 7. Section 8 includes suggestions for further validation and development of the IDBO scheme.

2 Principles of the Rigorous DBO Technique

This section draws heavily on the work of Maystre [1]. It is included to establish notation and to familiarise the reader with the nature of the method.

Consider the scattering of a plane electromagnetic wave incident normally upon an infinitely long cylindrical body situated in free space, as shown in Fig.1. The z-axis is chosen to be parallel to the axis of the cylinder. A general point on the surface contour C will have arc length s from a reference point P.

The body will be assumed to be perfectly conducting. The incident radiation is assumed time-harmonic. All fields will then exhibit the same time dependence, chosen to be $e^{-i\omega t}$, which will be suppressed throughout. We confine the analysis to the case where the incident electric field is z-polarised. (This case is also commonly referred to as E-polarisation or TM-polarisation.) Then the total electric field everywhere has a non-zero z-component only. At a point external to the scatterer with position vector $\underline{r}$ this is given by

$$E(\underline{r}) = E^i(\underline{r}) + E^s(\underline{r}), \tag{1}$$

where $E^i(\underline{r})$ and $E^s(\underline{r})$ denote the incident and scattered fields respectively. The scattered field satisfies the Helmholtz equation

$$(\nabla^2 + k^2)E^s(\underline{r}) = 0, \tag{2}$$

where $k^2 = \omega^2\mu_0\epsilon_0$ and μ_0 and ϵ_0 are respectively the permeability and permittivity of free space. In addition the scattered field is subject to the boundary condition

$$E^s|_C = -E^i|_C \tag{3}$$

on the surface C and to the far-zone Sommerfeld radiation condition.

The above completely specifies a physical electromagnetic scattering problem and in principle a unique solution for the electric field may be obtained. Often the surface current density $J(s)$ is determined first. The scattered field outside the body is then calculated by means of the Helmholtz representation :

$$E^s(\underline{r}) = -\int_C G(\underline{r},\underline{r}')j(\underline{r}')ds', \tag{4}$$

where $\underline{r}' = \underline{r}'(s')$ is the position vector of a general point on the contour C, $j = -i\omega\mu_0 J$ represents a normalised current density and the two-dimensional Green's function is given by

$$G(\underline{r},\underline{r}') = \frac{i}{4}H_0^{(1)}(k|\underline{r} - \underline{r}'|). \tag{5}$$

Now consider the following abstract problem — called the delta boundary operator (DBO) problem by Maystre. A fictitious source outside the scatterer is assumed

to be such that it gives rise to an incident field U^i of unit amplitude at a point $s = s_0$ on the surface of the body and which vanishes elsewhere on C; i.e.

$$U^i|_C = \delta(s - s_0). \tag{6}$$

(See Fig.2.) The presence of the scattering object causes a scattered field U^s which satisfies the following conditions :

$$(\nabla^2 + k^2)U^s(\underline{r}) = 0 \quad \text{outside } C \tag{7}$$

$$U^s|_C = -\delta(s - s_0). \tag{8}$$

In addition the scattered far-field must obey the appropriate radiation condition. The DBO problem, as stated here, is simply a mathematical boundary value problem. A unique solution for the scattered field is possible in principle.

Maystre defines a so-called ψ-distribution for the DBO problem which is analogous to the current j of the physical problem:

$$\psi(s, s_0) \equiv \frac{\partial U^s}{\partial n}(s, s_0). \tag{9}$$

The solution of the physical scattering problem may be obtained from that of the DBO problem by means of the principle of superposition. The required superposition is found by inspection of the boundary conditions (3) and (8) and by use of the relation

$$E^i(s) = \int_C \delta(s - s_0)E^i(s_0)ds_0. \tag{10}$$

For example, the scattered field on the surface of the scatterer is given by

$$E^s(s) = \int_C U^s(s, s_0)E^i(s_0)ds_0 = -E^i(s) \tag{11}$$

as required. Similarly the current $j(s)$ is given by

$$j(s) = \frac{\partial E^i}{\partial n}(s) + \int_C \psi(s, s_0)E^i(s_0)ds_0. \tag{12}$$

Thus the physical scattering problem may be solved by first solving the associated DBO problem to obtain the ψ-distribution.

It is important to appreciate that the rigorous DBO method of solution of a scattering problem offers nothing more than an alternative analysis. It is not anticipated that application of the method will lead to new exact analytic results for previously unsolved problems. As will become clear in Section 3 the value of this approach is that it suggests approximate techniques which are expected to be both fast and accurate for many scattering problems. With this in mind we now demonstrate the DBO method by applying it to two simple problems with known solutions.

2.1 Scattering by an infinite perfectly conducting plane

The plane is taken to be coincident with the $y = 0$ plane. We consider radiation in the region $y > 0$. The DBO problem is specified as follows :

$$(\nabla^2 + k^2)U^s(x,y) = 0 \quad \text{for } y > 0 \tag{13}$$

$$U^s(x,0) = -\delta(x - x_0) \tag{14}$$

$$U^s(x,y) \text{ satisfies a radiation condition as } y \to +\infty. \tag{15}$$

To obtain a solution we express U^s as a Fourier integral :

$$U^s(x,y) = \int_{-\infty}^{\infty} V(y,h)e^{ihx}dh. \tag{16}$$

Substitution into the Helmholtz equation gives

$$\frac{d^2V}{dy^2} + (k^2 - h^2)V = 0 \quad \text{for } y > 0. \tag{17}$$

The solution for V which ensures compliance with the radiation condition is

$$V(y,h) = V(0,h)e^{-\gamma(h,k)y}, \tag{18}$$

with

$$\gamma(h,k) = \begin{cases} (h^2 - k^2)^{1/2} & \text{for } |h| > k \\ -i(k^2 - h^2) & \text{for } |h| < k. \end{cases} \tag{19}$$

By using the relation

$$\delta(x - x_0) = \frac{1}{2\pi}\int_{-\infty}^{\infty} e^{ih(x-x_0)}dh \tag{20}$$

imposition of the boundary condition (14) gives

$$V(0,h) = -\frac{1}{2\pi}e^{-ihx_0}. \tag{21}$$

Thus we deduce

$$U^s(x,y) = -\frac{1}{2\pi}\int_{-\infty}^{\infty} e^{ih(x-x_0)}e^{-\gamma(h,k)y}dh. \tag{22}$$

In particular the ψ-distribution for this problem (denoted ψ^p) is given by

$$\psi^p(x,x_0) \equiv \frac{\partial U^s}{\partial y}(x,0) = \frac{1}{2\pi}\int_{-\infty}^{\infty} \gamma(h,k)e^{ih(x-x_0)}dh. \tag{23}$$

Manipulations with the Fourier transforms of Hankel functions allow closed form evaluation of this integral [1,7]. We find

$$\psi^p(x,x_0) = -\frac{ik}{2}\frac{H_1^{(1)}(k(x - x_0))}{(x - x_0)}. \tag{24}$$

Observe that $\psi^p(x, x_0)$ depends only on $x - x_0$, a consequence of the translation invariance of the scatterer. For a general cylindrical body Maystre [1] has shown that the ψ-distribution is a symmetric function; i.e.

$$\psi(s, s_0) = \psi(s_0, s). \tag{25}$$

This is a manifestation of the reciprocity principle.

Now consider the problem of scattering of a plane wave incident in the $x - y$ plane at an angle α to the surface normal. We have

$$E^i(x, y) = e^{ik(x\sin\alpha - y\cos\alpha)}. \tag{26}$$

Then the current is found from (2) to be

$$\begin{aligned} j(x) &= -ik\cos\alpha\, e^{ikx\sin\alpha} - \frac{ik}{2}\int_{-\infty}^{\infty} \frac{H_1^{(1)}(k(x - x_0))}{(x - x_0)} e^{ikx_0\sin\alpha} dx_0 \\ &= -2ik\cos\alpha\, e^{ikx\sin\alpha}, \end{aligned} \tag{27}$$

in accord with the well-known solution. Here use has been made of the Fourier transform of the Hankel function :

$$\int_{-\infty}^{\infty} \frac{H_1^{(1)}(kx)}{x} e^{ihx} dx = \frac{2i}{\kappa}\gamma(h, k). \tag{28}$$

2.2 Scattering by a perfectly conducting circular cylinder

The circular symmetry of this scatterer implies a ψ-distribution $\psi^c(s, s_0)$ dependent only on $s - s_0$. Without loss of generality we may thus set s_0 to zero and determine $\psi^c(s, 0)$.

For a cylinder of radius a, $s = a\theta$ and the DBO problem may therefore be stated as follows :

$$(\nabla^2 + k^2)U^s(r, \theta) = 0 \quad \text{for } r > a \tag{29}$$

$$U^s(a, \theta) = -\delta(\theta)/a \tag{30}$$

$$U^s(r, \theta) \text{ satisfies a radiation condition as } r \to \infty. \tag{31}$$

A straightforward calculation [1] produces the result

$$\psi^c(s, 0) = -\frac{k}{2\pi a}\sum_{n=-\infty}^{\infty} \frac{H_n^{(1)\prime}(ka)}{H_n^{(1)}(ka)} e^{ins/a}. \tag{32}$$

For a plane wave incident from the $+x$-direction (see Fig.3)

$$E^i(r, \theta) = e^{-ikr\cos\theta} \tag{33}$$

and (12) gives the surface current

$$j(a\theta) = \frac{\partial E^i}{\partial r}(a,\theta) + a\int_0^{2\pi} \psi^c(a\theta, a\theta_0)E^i(a,\theta_0)d\theta_0. \tag{34}$$

By expressing E^i as a Fourier series :

$$E^i(r,\theta) = \sum_{n=-\infty}^{\infty} (-i)^n J_n(kr)e^{-in\theta} \tag{35}$$

it can be readily verified that

$$j(a\theta) = -\frac{2i}{ka}\sum_{n=-\infty}^{\infty} \frac{(-i)^n}{H_n^{(1)}(ka)}e^{in\theta}. \tag{36}$$

Thus the classical solution is reproduced. (See, for example, Ref.8.)

3 Principles of the Approximate DBO (ADBO) Technique

Maystre [1] has performed analytical and numerical studies of the functions $\psi^c(s,0)$ and $\psi^p(s,0) = (-ik/2s)H_1^{(1)}(ks)$. His main observations are listed below :

1. $\psi^p(s,0)$ and $\psi^c(s,0)$ exhibit identical singularities as $s \to 0$. (Note however that $\psi^c(s,0)$ is a $2\pi a$-periodic function and so is singular as $s \to 2m\pi a$, where m is an integer. We limit comparison to the region $k|s| \leq \pi ka$.)

2. $\psi^c(s,0) \to \psi^p(s,0)$ as $ka \to \infty$.

3. Provided $ka \gtrsim 2$, $\psi^c(s,0) \approx \psi^p(s,0)$ for $k|s| \lesssim \pi ka$.

4. Values of both the real and imaginary parts of $\psi^p(s,0)$ become negligible for $k|s| \gtrsim 2\pi$.

5. Values of both the real and imaginary parts of $\psi^c(s,0)$ become negligible for $k|s| \gtrsim 2\pi$ provided $ka \gtrsim 2$.

Recalling the relationship (12) between the ψ-distribution and the surface current, observations 4 and 5 suggest the following fundamental conclusion [1,3] for TM incidence on a general $2D$ scatterer: *The surface current at any point on the body is influenced by the shape of the scatterer within a distance along the surface of approximately a wavelength.* This phenomenon of short-range coupling is excluded from the more popular Physical Optics (PO) theory which gives rise to surface currents which depend only on the *local* slope of the surface.

The observed similarities between the distributions $\psi^p(s,0)$ and $\psi^c(s,0)$ (for $ka \gtrsim 2$) suggest an approximate analysis of scattering by a general $2D$ body which accounts for the effects of short-range coupling. For a scatterer of perimeter l it seems reasonable to expect (and assume) that the true ψ-distribution $\psi(s,s_0)$ (which will be an l-periodic function in both s and s_0) can be accurately represented by the function $\psi^p(s,s_0)$ when $|s-s_0| \leq l/2$. This we shall call the approximate DBO (ADBO) approach. Underlying this assumption are two quite separate approximations:

1. It is assumed that $\psi(s,s_0)$ depends on the variables s and s_0 solely through their difference $s-s_0$; i.e. we assume $\psi(s,s_0) \approx \psi(s-s_0,0)$. This is certainly justifiable for bodies with surfaces which are small perturbations on a plane or circular cylinder but the validity of its wider applicability is uncertain.

2. It is assumed that $\psi(s-s_0,0) \approx \psi^p(s-s_0,0) = \psi_p(s,s_0)$ for $|s-s_0| \leq l/2$. In view of observations 1 and 3 on the ψ-distribution of the circular cylinder, it seems reasonable to anticipate that this approximation will introduce little error provided the scatterer is smooth (i.e. edges are absent) and is not too small; i.e. $l \gtrsim 2\lambda$ or $kl \gtrsim 4\pi$. ($\lambda = 2\pi/k$ denotes the wavelength of the exciting radiation.)

The assumption of a symmetric ψ-distribution ensures that fields obtained using this approximate technique obey the reciprocity principle. (See Section 2.) It is worth noting, though, that approximate solutions satisfying reciprocity may not be any more accurate than non-reciprocal ones [9].

Since $\psi(s, s_0)$ is l-periodic in s_0 (and s), (12) gives

$$j(s) = \frac{\partial E^i}{\partial n}(s) + \int_{s-l/2}^{s+l/2} \psi(s, s_0) E^i(s_0) ds_0. \tag{37}$$

Now, invoking approximation 1 above, we write

$$\begin{aligned} j(s) &\approx \frac{\partial E^i}{\partial n}(s) + \int_{s-l/2}^{s+l/2} \psi(s - s_0, 0) E^i(s_0) ds_0 \\ &= \frac{\partial E^i}{\partial n}(s) + \int_{-l/2}^{l/2} \psi(s', 0) E^i(s' + s) ds'. \end{aligned} \tag{38}$$

Implementation of approximation 2 then gives

$$j(s) \approx j_{ADBO}(s) \equiv \frac{\partial E^i}{\partial n}(s) + \int_{-l/2}^{l/2} \psi^p(s', 0) E^i(s' + s) ds'. \tag{39}$$

Recalling that $\psi^p(s, 0)$ is numerically negligible for $|s| \gtrsim \lambda$ (observation 4) we see that little loss of accuracy will ensue by changing the integration limits to $\pm\infty$; i.e.

$$j_{ADBO}(s) \approx \frac{\partial E^i}{\partial n}(s) + \int_{-\infty}^{\infty} \psi^p(s', 0) E^i(s' + s) ds'. \tag{40}$$

This further approximation is expected to be valid provided $l \gtrsim 2\lambda$.

The replacement of the true ψ-distribution by its counterpart for the plane may be viewed as an infinite plane approximation. PO uses an infinite tangent plane approximation to determine the current locally and the shape of the scatterer is accounted for when integrating the current to find the RCS. However, in the ADBO technique the infinite plane approximation is used one stage earlier, allowing the current to be influenced by the geometry of the scatterer in the nearby region.

It seems reasonable to expect (40) to be an accurate representation of reduced surface current on many $2D$ scatterers. Furthermore the current is expressed as a convolution-type integral which can be performed using Fourier transform techniques. Rapid calculation of currents can therefore be achieved by means of fast Fourier transform (FFT) algorithms. Since the Fourier transform of ψ^p is calculable analytically (see (28)) this procedure also alleviates problems which would be encountered in the direct numerical evaluation of the integral due to the singular behaviour of ψ^p.

In Refs.3 and 4 this approximate technique has been applied to scattering by planar rough surfaces. In the resonance region, where the roughness dimensions and

the wavelength of the incident radiation are of the same order of magnitude, the results were consistently more accurate than those obtained by using the Beckmann method [5,6], which strictly is applicable only when the wavelength is small relative to the scale of roughness. In Section 4 the application of the ADBO method to a simple smooth scatterer — the circular cylinder — is investigated in detail.

4 Application of ADBO Theory to Scattering by a Circular Cylinder

The scattering of a TM-polarised plane wave by a perfectly conducting circular cylinder has been examined rigorously in Section 2. Here the problem is revisited using the ADBO theory. From the arguments of the previous section we expect reasonable accuracy for $ka \gtrsim 2$. From (39) we find

$$j_{ADBO}(\theta) = -ik\cos\theta e^{-ika\cos\theta} - \frac{ik}{2} I_\pi(\theta, ka), \tag{41}$$

with

$$I_A(\theta, ka) = \int_{-A}^{A} \frac{H_1^{(1)}(ka\theta')}{\theta'} e^{-ika\cos(\theta'+\theta)} d\theta'. \tag{42}$$

As a first attempt at an analysis of the current we invoke the additional approximation $I_\pi(\theta, ka) \approx I_\infty(\theta, ka)$ in accordance with (40). For an approximate analytic evaluation of the integral I_∞ consider the following argument. From observation 4 of Section 3 we see that the distribution $H_1^{(1)}(ka\theta')/\theta'$ is numerically significant only when $|\theta'| \lesssim 2\pi/ka$. In view of this we are able to replace $e^{-ika\cos(\theta'+\theta)}$ by its small $|\theta'|$ approximation (strictly valid for $|\theta'| \ll 1$) when $ka \gg 2\pi$. Thus

$$\begin{aligned} I_\infty(\theta, ka) &\overset{ka\gg 2\pi}{\approx} e^{-ika\cos\theta} \int_{-\infty}^{\infty} \frac{H_1^{(1)}(ka\theta')}{\theta'} e^{ika\theta'\sin\theta} d\theta' \\ &= 2|\cos\theta| e^{-ika\cos\theta}, \end{aligned} \tag{43}$$

where use has been made of the standard integral (28). Therefore, when $ka \gg 2\pi$,

$$j_{ADBO}(\theta) \approx \begin{cases} -2ik\cos\theta e^{-ika\cos\theta} & \text{for } 0 \le |\theta| \le \pi/2 \\ 0 & \text{for } \pi/2 \le |\theta| \le \pi \end{cases} \tag{44}$$

These expressions for the reduced current on a conducting cylinder are precisely those predicted by PO theory. However, a more rigorous analysis of I_π is possible and is given in Appendix A. There it is found that

$$\begin{aligned} I_\pi(\theta, ka) \overset{ka\gg 1, \cos\theta\neq 0}{\approx} & 2|\cos\theta| e^{-ika\cos\theta} \left(1 + \frac{i}{2ka\cos^3\theta}\right) \\ & + I_\pi^t(\theta, ka) + I_\pi^{sp}(\theta, ka) \end{aligned} \tag{45}$$

where

$$I_\pi^t(\theta, ka) = \left(\frac{2}{ka}\right)^{3/2} \frac{e^{3i\pi/4} e^{i\pi ka} e^{ika\cos\theta}}{\pi^2 \cos^2\theta} \tag{46}$$

and

$$\begin{aligned} I_\pi^{sp}(\theta, ka) \overset{ka\gg 1, \cos\theta\neq 0}{\approx} & U(|\theta| - \pi/2) \left(\frac{8\pi}{ka}\right)^{1/2} \left(\frac{2}{ka}\right)^{1/3} Ai(0) e^{-3i\pi/4} \\ & \left(\frac{e^{ika(3\pi/2 - |\theta|)}}{(3\pi/2 - |\theta|)^{3/2}} + \frac{e^{ika(|\theta| - \pi/2)}}{(|\theta| - \pi/2)^{3/2}}\right). \end{aligned} \tag{47}$$

$U(x)$ denotes the unit step function and $Ai(x)$ represents the Airy function. Therefore the ADBO theory gives the following expressions for the current on a circular cylinder:

$$j_{ADBO}(\theta) \overset{ka\gg 1,\cos\theta\neq 0}{\approx} \begin{cases} -2ik\cos\theta e^{-ika\cos\theta}\left(1+\frac{i}{4ka\cos^3\theta}\right) \\ -\frac{ik}{2}I_\pi^t(\theta,ka) & \text{for } 0\le|\theta|\lesssim\pi/2 \\ -2ik\cos\theta e^{-ika\cos\theta}\left(\frac{-i}{4ka\cos^3\theta}\right) \\ -\frac{ik}{2}\left(I_\pi^t(\theta,ka)+I_\pi^{sp}(\theta,ka)\right) & \text{for } \pi/2\lesssim|\theta|\le\pi \end{cases} \tag{48}$$

In accordance with (44) PO currents are recovered in the high frequency ($ka\to\infty$) limit. These results are valid provided $ka\gg 1$ and $\cos\theta\not\approx 0$. Therefore we have been unable to derive a simple analytic form for the current in the transition region $|\theta|\approx\pi/2$. Outside the shadow boundary region we have obtained expressions for correction terms to the PO currents which account for the effects of the nearby scatterer shape. It is of interest to compare (48) with the corresponding asymptotic form of the exact current $j_{EX}(\theta)$ [10]:

$$j_{EX}(\theta) \overset{ka\gg 1,\cos\theta\neq 0}{\approx} \begin{cases} -2ik\cos\theta e^{-ika\cos\theta}\left(1+\frac{i}{2ka\cos^3\theta}\right) \\ -ike^{i\pi/6}\left(\frac{2}{ka}\right)^{1/3}\sum_{n=1}^{\infty}\frac{\left(e^{i\nu_n(3\pi/2-\theta)}+e^{i\nu_n(3\pi/2+\theta)}\right)}{Ai'(-\alpha_n)(1-e^{2i\nu_n\pi})} & \text{for } 0\le|\theta|\lesssim\pi/2 \\ -ike^{i\pi/6}\left(\frac{2}{ka}\right)^{1/3}\sum_{n=1}^{\infty}\frac{\left(e^{i\nu_n(|\theta|-\pi/2)}+e^{i\nu_n(3\pi/2-|\theta|)}\right)}{Ai'(-\alpha_n)(1-e^{2i\nu_n\pi})} & \text{for } \pi/2\lesssim|\theta|\le\pi \end{cases} \tag{49}$$

The infinite series represent creeping wave contributions. We see that the curvature correction term in the illuminated region predicted by the ADBO method is of the correct form and so breaks down in similar circumstances to $j_{EX}(\theta)$. However its magnitude is half the true value. Note also that $I_\pi^{sp}(\theta,ka)$ clearly represents a creeping wave contribution to the ADBO current.

To check the validity of the analytic approximation (48) away from the vicinity of the shadow boundary a numerical evaluation of I_π is necessary. This can be accomplished only after careful treatment of the singularity at $\theta'=0$. The details are discussed in Appendix A. $I_\pi(\theta,ka)$ has been evaluated using (83). Alternatively, and as discussed at the beginning of this section, calculation of $I_\pi(\theta,ka)$ can proceed approximately through evaluation of $I_\infty(\theta,ka)$. (It is shown in Appendix A.1 that the difference $I_\infty(\theta,ka)-I_\pi(\theta,ka)$ is of order $0(1/ka)^{3/2}$ and therefore small relative to either I_∞ or I_π when $ka\gg 1$.) The integral I_∞ has been evaluated numerically in three different ways:

1. Through computation of the expression equivalent to (83) for $I_A(\theta, ka)$:

$$\begin{aligned} I_A(\theta, ka) = & - H_1^{(1)}(kaA)(e^{-ika\cos(A+\theta)} + e^{-ika\cos(A-\theta)}) \\ & - iH_0^{(1)}(kaA)(\sin(A+\theta)e^{-ika\cos(A+\theta)} + \sin(A-\theta)e^{-ika\cos(A-\theta)}) \\ & + i\int_{-A}^{A} H_0^{(1)}(ka\theta')e^{-ika\cos(\theta'+\theta)}\cos(\theta'+\theta)(1-ika\cos(\theta'+\theta))d\theta'. \end{aligned} \tag{50}$$

   Values of I_∞ have been obtained by examining I_A for convergence for large A.

2. By using Fourier transform techniques (since $I_\infty(\theta, ka)$ is a convolution type integral). The equivalent results are obtained directly by means of Fourier series. Upon using the identity (35) we find

$$\begin{aligned} I_\infty(\theta, ka) &= \sum_{n=-\infty}^{\infty} (-i)^n J_n(ka)e^{-in\theta}\int_{-\infty}^{\infty} \frac{H_1^{(1)}(ka\theta')}{\theta'}e^{-in\theta'}d\theta' \\ &= \frac{2i}{ka}\sum_{n=-\infty}^{\infty}(-i)^n\gamma(n, ka)J_n(ka)e^{-in\theta}, \end{aligned} \tag{51}$$

   where the standard integral (28) has been used. Summation of this series has been performed by rewriting it as

$$I_\infty(\theta, ka) = \frac{2i}{ka}\sum_{n=0}^{\infty}\epsilon_n(-i)^n\gamma(n, ka)J_n(ka)\cos n\theta, \tag{52}$$

   ($\epsilon_0 = 1, \epsilon_1 = \epsilon_2 = \cdots = 2$) and retaining sufficient terms in the sum to ensure convergence.

3. By using an FFT algorithm.

The results obtained by these three methods differ negligibly.

Plots of the variation of the magnitude and phase of the surface current with angle θ, as given by (41), are shown in Fig.4 for $ka = 5$ and $ka = 10$. Also shown are the results with I_π replaced by I_∞ and the analytic form (48) of the currents. As expected invoking the extra approximation $I_\pi \approx I_\infty$ introduces little error (particularly for large ka). It is clear also that (48) is indeed a valid representation of the ADBO cylinder current in the deep illuminated and deep shadow regions.

In Fig.5 the magnitude and phase of the cylinder current obtained using the ADBO technique (by numerical evaluation of I_π) are compared with the corresponding exact [10] and PO solutions. In general the ADBO currents compare favourably with the PO results. Unlike PO, application of the ADBO method leads to predictions of non-vanishing surface currents in unlit regions and smooth transition currents at shadow boundaries. However the ADBO currents display an erroneous

oscillatory variation with angle for $\theta \gtrsim \pi/2$ and their magnitudes are over-estimated in the deep shadow region.

We now turn to a determination of the scattered far-field (and hence the radar cross section (RCS)) using the ADBO technique. This is achieved by integration of the current around the contour of the scatterer as indicated in (4). For the case of the circular cylinder the scattered far-field is found to be

$$E^s(r,\theta) \overset{kr\to\infty}{\longrightarrow} \frac{-ia}{\sqrt{8\pi kr}} e^{i(kr-\pi/4)} \int_0^{2\pi} j(\theta') e^{-ika\cos(\theta'-\theta)} d\theta'. \tag{53}$$

Since we have been unable to derive a reliable analytic expression for the ADBO current at all points on the surface we revert to the form (41). Inserting into (53) and interchanging the order of integration in the second term gives

$$E^s(r,\theta) \overset{kr\to\infty}{\longrightarrow} \frac{-\pi ka}{\sqrt{8\pi kr}} e^{i(kr-\pi/4)} \{-2i\cos(\theta/2) J_1(2ka\cos(\theta/2)) + L_\pi(\theta, ka)\}, \tag{54}$$

where

$$L_A(\theta, ka) = \int_{-A}^{A} \frac{H_1^{(1)}(ka\theta')}{\theta'} J_0\left(2ka\cos\left(\frac{\theta'+\theta}{2}\right)\right) d\theta'. \tag{55}$$

The bistatic RCS $\sigma(\theta)$ is defined as

$$\sigma(\theta) \equiv \lim_{r\to\infty} 2\pi r \left|\frac{E^s(r,\theta)}{E^i(r,\theta)}\right|^2. \tag{56}$$

ADBO predictions of bistatic RCS are shown in Fig.6 for cylinders of size $ka = 5$ and $ka = 10$. Also shown are the corresponding exact [8] and PO results. As with I_π care has been taken with the singularity of the integrand for the numerical evaluation of L_π. There is evidence that the over-estimated currents in the deep shadow region contribute significantly to the RCS, with their erroneous oscillatory angular behaviour persisting after integration. It is debatable whether application of the ADBO technique to the circular cylinder scattering problem has led to improvements over the PO RCS predictions.

In view of this disappointing conclusion it is natural to ask how the ADBO scheme might be modified to improve its accuracy. The two basic assumptions inherent in the technique were given in Section 3. It has already been remarked that the ψ-distribution for the cylinder $\psi^c(s, s_0)$ depends only on $s - s_0$; i.e. $\psi^c(s, s_0) = \psi^c(s - s_0, 0)$. Thus only the second approximation was used in the cylinder analysis; i.e. we assumed $\psi^c(s, 0) \approx \psi^p(s, 0)$ for $|s| \leq \pi a$. Although observation 3 of Section 3 supports this assumption it is clear that it is inadequate for the cases we have considered ($ka = 5$ and $ka = 10$). It seems likely that a better approximation to $\psi^c(s, 0)$ will lead to improved current and RCS predictions. Therefore in Section 5 we examine in detail the ψ-distribution of the circular cylinder.

5 Analysis of the ψ-Distribution of the Circular Cylinder

In this section we seek an improved approximation for $\psi^c(s,0)$. Since $\psi^c(s,0) \rightarrow \psi^p(s,0)$ as $ka \rightarrow \infty$ (observation 2 of Section 3) we look for correction terms by examining the asymptotic behaviour of the exact expression (32). By using a Watson transformation (see Appendix B) we find

$$\psi^c(s,0) \overset{ka \gtrsim 1}{\approx} \psi^p(s,0) - \frac{ik}{4a} e^{ik|s|} + \psi^{c(2)}(s,0), \tag{57}$$

where

$$\psi^{c(2)}(s,0) = \frac{ik}{a} \sum_{n=1}^{\infty} \sum_{m=1}^{\infty} (e^{i\nu_n(2m\pi+\theta)} + e^{i\nu_n(2m\pi-\theta)}), \tag{58}$$

with

$$\theta = \frac{s}{a}. \tag{59}$$

$\psi^{c(2)}(s,0)$ represents creeping wave contributions. For each value of n (corresponding to a root ν_n of $H^{(1)}_{\nu_n}(ka) = 0$) there is an infinite number of such terms, each integral change in m corresponding to a complete circulation of the cylinder. However, careful inspection shows that not all of the expected creeping wave terms are present. Recalling that $|\theta| \leq \pi$ we see in particular that all waves emanating from the point of excitation on the surface and traversing less than half the cylinder circumference are excluded. Indeed $\psi^{c(2)}(s,0)$ offers a complete representation of creeping waves only when $\theta = 0$. The imaginary parts of the ν_n determine the rates at which the creeping waves are attenuated as they move around the cylinder. From (135), $Im(\nu_n) \propto (ka)^{1/3}$ and so for large ka there is considerable attenuation. Bearing in mind the remarks made above it follows that the most significant creeping wave contributions are excluded from $\psi^{c(2)}(s,0)$. Indeed, even for moderate values of ka it is readily verified using (135) and tables of the constants α_n (see, for example, Ref.11) that

$$|e^{i\nu_n(2m\pi+\theta)}|, \quad |e^{i\nu_n(2m\pi-\theta)}| \lesssim 10^{-4}. \tag{60}$$

for all allowed values of m and n. It is immediately apparent that the contribution of $\psi^{c(2)}(s,0)$ to $\psi^c(s,0)$ is relatively small and indeed numerically negligible. Thus in our numerical investigation of (57) we will ignore the contribution of $\psi^{c(2)}(s,0)$. We must however anticipate that the issue of the 'missing' creeping waves is an important one since their numerical contributions may be significant. This matter will be discussed again later in this section.

The validity of (57) and the significance of the curvature correction term can be determined by numerical comparison with the exact form (32) and the plane approximation $\psi^p(s,0)$. Maystre [1] has rewritten (32) in a form suitable for computation:

$$\frac{2\pi}{k^2}\psi^c(s,0) = -\frac{1}{2(ka)^2\sin^2(\theta/2)} + \ln 2\cos\theta + \frac{(\pi-|\theta|)}{2}\sin|\theta|$$
$$+ \cos\theta \ln|\sin(\theta/2)| + \frac{1}{ka}\frac{H_1^{(1)}(ka)}{H_0^{(1)}(ka)} - \frac{2}{ka}\frac{H_0^{(1)}(ka)}{H_1^{(1)}(ka)}\cos\theta$$
$$- \sum_{n=2}^{\infty}\frac{1}{n-1}\frac{H_{n-2}^{(1)}(ka)}{H_n^{(1)}(ka)}\cos n\theta. \qquad (61)$$

The infinite series converges rapidly. As before $\theta = s/a$ and $|\theta| \leq \pi$. Plots of the real and imaginary parts of $\psi^c(s,0)$ are given in Fig.7 for the cases $ka = 5$ and $ka = 10$. Also shown is the plane approximation $\psi^p(s,0)$ and the approximation to $\psi^c(s,0)$ given by (57). Two remarks are appropriate:

1. The discrepancies between $\psi^p(s,0)$ and the exact form (61) of $\psi^c(s,0)$ are sufficiently large to support our conclusion that the ADBO procedure is inadequate for accurate current and RCS predictions.

2. The inclusion of the curvature correction leads to a significant improvement to our approximation to $\psi^c(s,0)$ only for $k|s| \lesssim 1$.

It is apparent from Fig.7 that the representation (57) of $\psi^c(s,0)$ fails for $k|s| \gtrsim 1$. This is because the magnitude of the curvature correction does not decrease with increasing $k|s|$. It is this term which dominates for $k|s| \gtrsim 1$ giving rise to the observed oscillatory behaviour. Clearly for a more accurate representation of $\psi^c(s,0)$ this correction term must be strongly damped as $k|s|$ is increased. The origin of the absent attenuation is alluded to in Appendix B. There it is noted that the approximation (132) to $f(\nu,ka) = H_\nu^{(1)\prime}(ka)/H_\nu^{(1)}(ka)$ (used to determine (57)) does not have the correct pole structure. Nevertheless (132) *is* a good approximation to $f(\nu,ka)$ provided $|\nu| \not\approx ka$. In particular it is valid when $|\nu| \gg ka$. That this is so is borne out by the accuracy of the representation (57) of $\psi^c(s,0)$ for $k|s| \lesssim 1$, since the variables $\frac{\nu}{ka}$ and ks form a Fourier transform pair.

To obtain a more accurate model of $\psi^c(s,0)$ for $k|s| \gtrsim 1$ we must invoke a representation for $f(\nu,ka)$ which has the correct behaviour when $|\nu| \approx ka$. In particular we require that $f(\nu,ka)$ has poles at $\nu = \pm\nu_n$ (since, by (128), $f(\nu,ka) = f(-\nu,ka)$). The residues associated with the poles at $\nu = \nu_n$ are given by

$$\lim_{\nu\to\nu_n}(\nu-\nu_n)f(\nu,ka) = \frac{H_{\nu_n}^{(1)\prime}(ka)}{\frac{\partial}{\partial\nu}H_\nu^{(1)}(ka)|_{\nu=\nu_n}}$$
$$\overset{ka\gg 1}{\approx} -1, \qquad (62)$$

by (153). Thus we write

$$f(\nu,ka) \overset{|\nu|\approx ka\gg 1}{\approx} -\frac{\gamma(\nu,ka)}{ka} - \sum_{n=1}^{\infty}\left(\frac{1}{\nu-\nu_n} - \frac{1}{\nu+\nu_n}\right)$$

$$= \quad -\frac{\gamma(\nu, ka)}{ka} - 2\sum_{n=1}^{\infty} \frac{\nu_n}{(\nu^2 - \nu_n^2)}. \tag{63}$$

Following similar arguments to those which lead to (138) we find that use of this expression gives the following approximate representation of $\psi^c(s,0)$:

$$\begin{aligned} \psi^c(s,0) &\overset{ka\gtrsim 1}{\approx} \psi^p(s,0) + \frac{i}{a^2}\sum_{n=1}^{\infty} \nu_n e^{i\nu_n|\theta|} \\ &\overset{ka\gtrsim 1}{\approx} \psi^p(s,0) + \frac{ik}{a}\sum_{n=1}^{\infty} e^{i\nu_n|\theta|}. \end{aligned} \tag{64}$$

We expect this model to be reasonably accurate for $k|s| \gtrsim 1$. Since $Im(\nu_n) > 0$ and $Im(\nu_n) \propto (ka)^{1/3}$ the curvature correction term is strongly attenuated as $k|s|$ is increased. Indeed, upon inspection of (58) and (64) it is apparent that this term represents the so-called 'missing' creeping waves referred to earlier in this section. They are numerically significant since they traverse less than half the cylinder circumference. Although we expect the representation (64) to be satisfactory for $k|s| \gtrsim 1$ it is clear that it breaks down for $k|s| \ll 1$. Indeed, as $|s|$ (or equivalently $|\theta|$) approaches zero the imaginary part of the correction term blows up, a feature not present in plots of the exact form of $\psi^c(s,0)$.

It is worth making a comment here on the analysis of $\psi^c(s,0)$ given in Appendix B. Although the split into two components $\psi^{c(1)}$ and $\psi^{c(2)}$ (through use of (130)) is mathematically convenient it is not unique and it does not lead to separation of physically distinct contributions as it does in the analysis of the scattering of a plane wave by a circular cylinder [11]. In particular creeping waves appear in the analysis of both components. It is quite possible that a different split would be justifiable on physical grounds.

So far in this section two simple representations ((57) and (64)) of the ψ-distribution of the circular cylinder have been obtained. They have been shown to be valid for different values of $k|s|$. Ideally we would like a single expression accurate throughout the interval $0 \leq k|s| \leq \pi ka$. Maystre [1] has given an empirical formula which is able to represent $\psi^c(s,0)$ to a very high degree of precision. It appears that this was obtained by performing a seven parameter study using limited information on the expected analytic form. As a result Maystre's formula is complicated and may not be readily applicable to other smooth scatterers. The present author has attempted a rigorous analysis of the exact form of $\psi^c(s,0)$ in a bid to discover a simple and accurate representation. The fact that this approach failed to produce a single usable form is directly traceable to the absence of an analytic expression for the Fourier transform of $H_\nu^{(1)\prime}(z)/H_\nu^{(1)}(z)$ (with respect to ν) accurate for all real ν and z. Nevertheless, as we shall now demonstrate, it is possible to produce a very good approximation to $\psi^c(s,0)$ for $0 \leq k|s| \leq \pi ka$ using a simple single parameter model. This is achieved by making use of much of the information gleaned from the

rigorous analysis. Specifically, we postulate

$$\psi^c(s,0) \overset{ka\gg 1}{\approx} \psi^p(s,0) - \frac{ik}{4a} e^{i\nu_0|\theta|}, \tag{65}$$

with

$$\nu_0 = ka + \alpha_0 (ka/2)^{1/3} e^{i\pi/3}. \tag{66}$$

The correction term has been chosen to ensure accuracy for $k|s| = ka|\theta| \ll 1$ and to represent the combined effect of the creeping waves traversing less than half the cylinder circumference. When the parameter α_0 takes the value 0.55, (65) is an accurate representation for $0 \leq k|s| \leq \pi ka$. This is demonstrated in Fig.8 for $ka = 5$ and $ka = 10$. Fine tuning of α_0 may lead to even better agreement with the exact form. Computation of the cylinder current using (65) (which we shall call the improved DBO (IDBO) approximation) is described in the next section.

6 Application of IDBO Theory to Scattering by a Circular Cylinder

The scattering of a TM-polarised plane wave by a perfectly conducting circular cylinder has been examined rigorously in Section 2 and using ADBO theory in Section 4. The currents obtained by applying the ADBO technique were found to be inaccurate in the shadow region. Here the problem is revisited using the improved form of the ψ-distribution for the circular cylinder obtained in Section 5. From (38) and (65) we find

$$j_{IDBO}(\theta) = -ik\cos\theta e^{-ika\cos\theta} - \frac{ik}{2}I_\pi(\theta, ka) - \frac{ik}{4}M_\pi(\theta, ka), \tag{67}$$

with

$$M_A(\theta, ka) = \int_{-A}^{A} \epsilon^{i\nu_0|\theta'|}\epsilon^{-ika\cos(\theta'+\theta)}d\theta'. \tag{68}$$

The integral M_π can be analysed using asymptotic techniques. (See Appendix C.) It is found that

$$M_\pi(\theta, ka) \overset{ka\gg 1, \cos\theta\neq 0}{\approx} \frac{2i\nu_0 e^{-ika\cos\theta}}{(\nu_0^2 - (ka)^2\sin^2\theta)} + M_\pi^t(\theta, ka) + M_\pi^{sp}(\theta, ka), \tag{69}$$

where

$$M_\pi^t(\theta, ka) = -\frac{2i\nu_0\epsilon^{i\nu_0\pi}e^{ika\cos\theta}}{(\nu_0^2 - (ka)^2\sin^2\theta)} \tag{70}$$

and

$$M_\pi^{sp}(\theta, ka) \overset{ka\gg 1}{\approx} U(|\theta| - \pi/2)2\pi\left(\frac{2}{ka}\right)^{1/3} Ai(\alpha_0\epsilon^{i\pi/3})(e^{i\nu_0(|\theta|-\pi/2)} + \epsilon^{i\nu_0(3\pi/2-|\theta|)}). \tag{71}$$

Since $\nu_0 \approx ka$ for $ka \gg 1$ and using also the result (48) for $j_{ADBO}(\theta)$, it follows that

$$j_{IDBO}(\theta) \overset{ka\gg 1, \cos\theta\neq 0}{\approx} \begin{cases} -2ik\cos\theta e^{-ika\cos\theta}\left(1 + \frac{i}{2ka\cos^3\theta}\right) & \\ -\frac{ik}{2}I_\pi^t(\theta, ka) - \frac{ik}{4}M_\pi^t(\theta, ka) & \text{for } 0 \leq |\theta| \lesssim \pi/2 \\ -\frac{ik}{2}(I_\pi^t(\theta, ka) + I_\pi^{sp}(\theta, ka)) & \\ -\frac{ik}{4}(M_\pi^t(\theta, ka) + M_\pi^{sp}(\theta, ka)) & \text{for } \pi/2 \lesssim |\theta| \leq \pi \end{cases} \tag{72}$$

Several comments are appropriate:

1. Comparing (72) with the asymptotic form of the exact current $j_{EX}(\theta)$ (49) we see that IDBO theory yields the correct curvature correction to the PO current in the illuminated region. Furthermore the erroneous curvature correction term present in $j_{ADBO}(\theta)$ for $\pi/2 \lesssim |\theta| \leq \pi$ is precisely cancelled by a contribution of similar form due to $M_\pi(\theta, ka)$.

2. The I_π^{sp} and M_π^{sp} terms together generate an approximate representation of the most significant creeping wave contributions to the current on the shadowed side of the cylinder. In Section 5 it was observed that creeping waves traversing more than half the cylinder circumference were severely attenuated and gave ar insignificant numerical contribution to the DBO ψ-distribution. Their contribution was therefore neglected. Thus no creeping wave terms are present in the IDBO prediction of the current in the lit region. In Appendix D it is confirmed that the correct creeping wave behaviour for $|\theta| \lesssim \pi/2$ is generated by retaining the term $\psi^{c(2)}(s,0)$ (58) in the approximate representation of $\psi^c(s,0)$. Likewise all higher order creeping wave contributions to the current in the shadow region are produced.

3. The I_π^t and M_π^t terms are present because the approximation (65) provides an inadequate model of $\psi^c(s,0)$ for $s \approx \pm\pi a$. This is not a serious concerr because even for moderate ka they are numerically very small.

It has already been confirmed in Section 4 that the substitution of I_∞ for I_π in (41) makes little numerical difference. In a similar way, and in particular because $Im(\nu_0) > 0$, we expect that the replacement of M_π by M_∞ in (67) will introduce little error. Thus we write

$$j_{IDBO}(\theta) \overset{ka\gg 1}{\approx} -ik\cos\theta e^{-ika\cos\theta} - \frac{ik}{2} I_\infty(\theta, ka) - \frac{ik}{4} M_\infty(\theta, ka) \tag{73}$$

and we may employ FFT techniques for an efficient computation of I_∞ and M_∞. In a combined evaluation of the second and third terms on the right side of (73) use can be made of the analytic form for the Fourier transform of our approximation (65) to $\psi^c(s,0)$:

$$\begin{aligned} \tilde{\psi}^c(\omega) &\equiv \int_{-\infty}^{\infty} \psi^c(a\theta, 0) e^{i\omega\theta} d\theta \\ &\overset{ka\gg 1}{\approx} \frac{\gamma(\omega, ka)}{a} + \frac{k}{2a} \frac{\nu_0}{(\nu_0^2 - \omega^2)}. \end{aligned} \tag{74}$$

Note that, since $Im(\nu_0) > 0$, the second term is not singular for real ω. (Recalling that (65) was derived in an attempt to approximate the Fourier transform of $f(\nu, ka)$ with respect to ν we expect a better approximation to $\tilde{\psi}^c(\omega)$ to be given by

$$\tilde{\psi}^c(\omega) \approx -kf(\omega, ka) = -k \frac{H_\omega^{(1)\prime}(ka)}{H_\omega^{(1)}(ka)}. \tag{75}$$

However, this result is likely to be less readily generalisable for application to an arbitrary smooth scatterer.)

Plots of the magnitude and phase of the surface current, as given by (67), are shown in Fig.9 for $ka = 5$ and $ka = 10$. The integrals I_π and M_π have been evaluated

numerically. Also shown are the results obtained using (73) and the analytic form (72). As expected invoking the extra approximations $I_\pi \approx I_\infty$ and $M_\pi \approx M_\infty$ introduces little error. It is also clear that (72) is indeed a valid representation of the cylinder current obtained using the IDBO technique away from the region of the shadow boundary.

In Fig.10 the cylinder currents obtained by the IDBO method are compared with the corresponding exact and PO solutions. In general the IDBO currents are much more accurate than those of PO at all points on the cylinder surface. There is, however, some residual erroneous oscillatory variation with angle in the shadowed region.

7 Prescription of the IDBO Technique for a General Two-Dimensional Smooth Scatterer

In Section 6 the IDBO method was successfully applied to the problem of plane wave scattering by a perfectly conducting circular cylinder. This should not have surprised us since the technique was based upon a derivation of an accurate approximation to the known ψ-distribution for that scatterer. The technique can only be used to advantage when its validity has been demonstrated for bodies for which the exact ψ-distribution is *not* known. Only then will the procedure yield a true predictive capability.

The simple approximation (65) to $\psi^c(s,0)$ was developed with the aim of being readily generalisable for application to an arbitrary $2D$ smooth scatterer. We therefore postulate the following form for the ψ-distribution of such a body:

$$\psi_{IDBO}(s_1,s_2) = \psi^p(s_1,s_2) - \frac{ik}{4a(s_1,s_2)} e^{ik|s_1-s_2|} e^{i\alpha_0 e^{i\pi/3}|\xi(s_1,s_2)|} \tag{76}$$

where $\alpha_0 = 0.55$ and s_1 and s_2 denote the arc lengths of points P_1 and P_2 on the scatterer surface from some reference point also on that surface. This expression is sufficiently general to allow dependence on both variables s_1 and s_2 rather than just the single quantity $s_1 - s_2$. We have yet to prescribe the functions $a(s_1,s_2)$ and $\xi(s_1,s_2)$. Any proposed form for $a(s_1,s_2)$ should reduce to the constant value a for the case of a circular cylinder of radius a while $|\xi(s_1,s_2)|$ should reduce to $(k/2a^2)^{1/3}|s_1 - s_2|$.

To obtain suitable expressions for $a(s_1,s_2)$ and $\xi(s_1,s_2)$ we appeal to Fock theory. In the application of Fock theory to a general convex body [11] it is seen that the amplitude of the current in the shadow region depends only on the radii of curvature of the surface at the point of excitation (P_1 say) of the creeping wave and at the point of observation (P_2) and also on the quantity

$$\int_{s_1}^{s_2} \left(\frac{k}{2a^2(s')}\right)^{1/3} ds', \tag{77}$$

where $a(s)$ is the radius of curvature as a function of arc length. Thus, in order also to preserve symmetry under interchange of s_1 and s_2, we propose that

$$a(s_1,s_2) = \sqrt{a(s_1)a(s_2)}, \tag{78}$$

and

$$\xi(s_1,s_2) = \int_{s_1}^{s_2} \left(\frac{k}{2a^2(s')}\right)^{1/3} ds'. \tag{79}$$

In accordance with (37) the IDBO prediction of the surface current induced by an incident field E^i on a closed body of perimeter l would be as follows:

$$j_{IDBO}(s) = \frac{\partial E^i}{\partial n}(s) + \int_{s-l/2}^{s+l/2} \psi_{IDBO}(s,s')E^i(s')ds'. \tag{80}$$

The form of the ψ-distribution given by (76),(78) and (79) has yet to be tested for any scatterer other than the circular cylinder. Suitable test targets would be the elliptic and parabolic cylinders for which control solutions are readily available. (See, for example, Ref.12).

For a general smooth body $a(s_1, s_2)$ and $\xi(s_1, s_2)$ will be complicated functions of both s_1 and s_2. Thus the contribution of the curvature correction term of ψ_{IDBO} to the current j_{IDBO} will not be amenable to rapid approximate calculation using FFT algorithms.

The prescribed forms (78) and (79) ensure that $\psi_{IDBO}(s_1, s_2)$ is symmetric and so the fields calculated using the IDBO scheme are guaranteed to comply with the reciprocity principle. (See [1] and Section 3.)

8 Conclusions and Suggestions for Further Work

In the DBO formulation of the electromagnetic scattering problem the current is expressed in the form of an integral over the scatterer surface with the integrand containing a so-called ψ-distribution which is characteristic of the scatterer and depends only on the polarisation of the incident radiation. The ψ-distribution gives the current induced at a point on the scatterer surface due to a delta-function excitation at a second such point. In this report two approximate techniques based on the DBO formulation have been examined. These schemes aim to provide accurate representations of the ψ-distribution. A simple approximation (the ADBO procedure) is to use the known ψ-distribution for the infinite plane. Although used successfully in the past to treat scattering by rough planar surfaces [3,4] we saw in Section 4 that it gives unsatisfactory predictions of current and bistatic RCS for circular cylinders in the resonance region. In particular it includes only half of the known curvature correction to the PO current in the illuminated region and over-estimates tha magnitude of the shadow region currents. An improved approximation was derived and applied to the circular cylinder problem. This IDBO scheme led to good agreement with the known current everywhere on the cylinder. A generalisation of the IDBO technique to allow treatment of scattering by arbitrary $2D$ smooth bodies was proposed in Section 7.

In general the approximate DBO techniques have the following features:

1. Unlike PO their application leads to predictions of non-vanishing surface currents in unlit regions and smooth transition currents at shadow boundaries.

2. Unlike PO they yield currents which do not depend solely on the local geometry of the scatterer; i.e. the currents are non-local. They make explicit the phenomenon of short-range coupling, demonstrating that the surface current at any point on the body is influenced by the shape of the scatterer within a distance along the surface of about a wavelength.

3. A single expression gives the surface current everywhere on the body. This contrasts with Fock's calculation of surface currents in the vicinity of the shadow boundary [11]. Interpolation formulae are required to extend Fock's results into the deep illumination region.

4. Provided that the assumed ψ-distribution is symmetric with respect to its arguments the calculated fields will comply with the reciprocity principle.

5. They are more efficient than, for example, integral equation techniques because the currents are given explicitly.

6. They are readily applicable for any incident field.

Any attempt to produce accurate current and field predictions using approximate DBO techniques must be based upon a reliable representation of the appropriate

ψ-distribution. It seems likely that an accurate model of the ψ-distribution for a general scatterer many wavelengths in size can be generated by gleaning information from the ψ-distributions of a small number of standard (canonical) bodies. This is the philosophy of the successful Geometrical Theory of Diffraction and is also the reasoning behind the in-depth investigation of the ψ-distribution of the circular cylinder in this paper. An IDBO treatment of scattering by bodies with edges requires an examination of the ψ-distribution of an infinite wedge. This work is well advanced and will be reported in a future paper. An alternative approach would be the approximate numerical computation of the ψ-distribution of an arbitrary scatterer by disregarding the (usually insignificant) influence of distant parts of the body.

In this paper we have been concerned only with the case of TM incidence on a perfectly conducting infinite cylindrical body. Provided that the IDBO technique is properly validated for this case it seems that further development of the technique to allow treatment of TE incidence, full $3D$ vector scattering and possibly scattering by dielectric and magnetic objects may be both feasible and beneficial.

9 References

1. D.Maystre; J. Mod. Optics, Vol.34, pp.1433-1450, 1987.

2. M.Saillard, A.Roger and D.Maystre; J. Mod. Optics, Vol.35, pp.1317-1330, 1988.

3. D.Maystre; IEEE Trans. Antennas Propagat., Vol.AP-31, pp.885-895, 1983.

4. A.Roger and D.Maystre; J. Mod. Optics, Vol.35, pp.1579-1589, 1988.

5. P.Beckmann and A.Spizzichino; 'The Scattering of Electromagnetic Waves from Rough Surfaces', New York, Pergamon, 1963.

6. P.Beckmann; 'Scattering of Light by Rough Surfaces', in Progress in Optics, Vol.VI, ed. E.Wolf, Amsterdam, North Holland, 1967.

7. B.Noble; 'Methods based on the Wiener-Hopf Technique', London, Pergamon, 1958, p.67.

8. G.T.Ruck (Ed.); 'Radar Cross Section Handbook', New York, Plenum, 1970, ch.4.

9. G.S.Brown; IEEE Trans. Antennas Propagat., Vol.AP-31, pp.992-993, 1983.

10. J.J.Bowman, T.B.A.Senior and P.L.E.Uslenghi (Eds.); 'Electromagnetic and Acoustic Scattering by Simple Shapes', Amsterdam, North-Holland, 1969, ch.2.

11. G.T.Ruck (Ed.); 'Radar Cross Section Handbook', New York, Plenum, 1970, ch.2.

12. J.J.Bowman, T.B.A.Senior and P.L.E.Uslenghi (Eds.); ibid., ch.3 & 7.

13. I.S.Gradshteyn and I.M.Ryzhik; 'Table of Integrals, Series and Products', London, Academic Press, 1980, p.955.

14. G.L.James; 'Geometrical Theory of Diffraction for Electromagnetic Waves', IEE Electromagnetic Waves Series 1, Peter Peregrinus, 1976, ch.2.

15. I.S.Gradshteyn and I.M.Ryzhik; ibid., p.345.

16. M.Abramowitz and I.A.Stegun; 'Handbook of Mathematical Functions', New York, Dover, 1965, pp.368-369.

17. G.L.James; ibid., ch.3.

18. D.S.Jones; 'Acoustic and Electromagnetic Waves', Oxford, Clarendon Press, 1986, Appendix A.

19. D.S.Jones; ibid., Appendix G.

Acknowledgement

The author wishes to thank Dr.P.L.Aspden of the Department of Electronic and Electrical Engineering, University of Sheffield for performing the calculations which used FFT algorithms.

A Analysis of the Integral $I_\pi(\theta, ka)$

The integral $I_\pi(\theta, ka)$ (Eq.(42)) occurs in the ADBO treatment of scattering by a conducting circular cylinder. Exact analytic evaluation of this integral appears not to be possible. Here we attempt an approximate evaluation for $ka \gg 1$.

The integrand of $I_\pi(\theta, ka)$ behaves as $(1/\theta')^2$ for $|\theta'| \ll 1$ and so it is not integrable in the usual sense. However, as discussed in detail by Maystre [3], integrals of this type arise in the DBO technique as derivatives of principal value integrals and so they are well-defined. Thus we write

$$I_\pi(\theta, ka) = \lim_{\epsilon \to 0} \left\{ \frac{4i}{\pi ka\epsilon} e^{-ika\cos\theta} + \left(\int_{-\pi}^{-\epsilon} + \int_{\epsilon}^{\pi} \right) \frac{H_1^{(1)}(ka\theta')}{\theta'} e^{-ika\cos(\theta'+\theta)} d\theta' \right\}. \quad (81)$$

To render $I_\pi(\theta, ka)$ in a form suitable for asymptotic analytic evaluation (and indeed numerical evaluation) we use Bessel's equation to give

$$I_\pi(\theta, ka) = \frac{1}{ka} \int_{-\pi}^{\pi} \left(\frac{d^2}{d\theta'^2} H_0^{(1)}(ka\theta') + (ka)^2 H_0^{(1)}(ka\theta') \right) e^{-ika\cos(\theta'+\theta)} d\theta' \quad (82)$$

and then integrate by parts to find

$$\begin{aligned} I_\pi(\theta, ka) = \quad & i \int_{-\pi}^{\pi} H_0^{(1)}(ka\theta') e^{-ika\cos(\theta'+\theta)} \cos(\theta'+\theta)(1 - ika\cos(\theta'+\theta)) d\theta' \\ - \quad & 2H_1^{(1)}(\pi ka) e^{ika\cos\theta}. \end{aligned} \quad (83)$$

The integrand of the remaining integral possesses a logarithmic singularity at $\theta' = 0$ and so is integrable in the conventional sense. Asymptotic analysis of this integral is most convenient through consideration of the integral $K_\pi(\theta, ka)$:

$$K_\pi(\theta, ka) \equiv \int_{-\pi}^{\pi} H_0^{(1)}(ka\theta') e^{-ika\cos(\theta'+\theta)} d\theta'. \quad (84)$$

Straightforward manipulation shows that $I_\pi(\theta, ka)$ may be expressed in terms of $K_\pi(\theta, ka)$ as follows:

$$I_\pi(\theta, ka) = -2H_1^{(1)}(\pi ka) e^{ika\cos\theta} + \frac{1}{ka} \frac{\partial^2 K_\pi(\theta, ka)}{\partial \theta^2} + ka\, K_\pi(\theta, ka). \quad (85)$$

When $ka \gg 1$ the function $H_0^{(1)}(ka\theta')$ is not slowly varying in the region $-\pi \leq \theta' \leq \pi$. However, asymptotic evaluation of $K_\pi(\theta, ka)$ can proceed by conventional techniques using the following integral representation [13]:

$$H_0^{(1)}(ka\theta') = \frac{1}{i\pi} \int_{-\infty}^{\infty} e^{ika|\theta'|\cosh t} dt. \quad (86)$$

Substituting into (84) and interchanging the order of integration gives

$$K_\pi(\theta, ka) = K_\pi^{(+)}(\theta, ka) + K_\pi^{(-)}(\theta, ka), \quad (87)$$

where

$$K_\pi^{(+)}(\theta, ka) = \frac{1}{i\pi}\int_{-\infty}^{\infty}\int_0^{\pi} e^{ikag_+(\theta',t)}d\theta' dt \tag{88}$$

$$K_\pi^{(-)}(\theta, ka) = \frac{1}{i\pi}\int_{-\infty}^{\infty}\int_{-\pi}^{0} e^{ikag_-(\theta',t)}d\theta' dt \tag{89}$$

$$g_\pm(\theta', t) = \pm\theta' \cosh t - \cos(\theta' + \theta). \tag{90}$$

A proper asymptotic analysis of these double integrals must account for both stationary phase point and end-point contributions. (See, for example, Ref.14.) These contributions are now considered in turn.

A.1 Stationary Phase Point Contributions

For evaluation of the stationary phase point contributions to $K_\pi(\theta, ka)$ it is convenient to note that K_π is even in θ ; i.e. $K_\pi(\theta, ka) = K_\pi(-\theta, ka)$, and therefore that the analysis can be confined to a treatment of the interval $0 \leq \theta \leq \pi$. Consider first the double integral $K_\pi^{(+)}(\theta, ka)$. For a stationary phase point at $(\theta', t) = (\theta_0', t_0)$ the following pair of simultaneous equations must be satisfied:

$$\cosh t_0 + \sin(\theta_0' + \theta) = 0 \tag{91}$$

$$\theta_0' \sinh t_0 = 0. \tag{92}$$

A solution is possible only when $t_0 = 0$ *and* $\sin(\theta_0' + \theta) = -1$. It follows that there is no stationary phase point contribution to $K_\pi^{(+)}(\theta, ka)$ in the interval $0 \leq \theta < \pi/2$. For $\pi/2 < \theta \leq \pi$, however, there *is* a stationary phase point in the integration interval $0 < \theta' < \pi$ at $\theta_0' = 3\pi/2 - \theta$. To evaluate its contribution, which we shall call $K_\pi^{(+)sp}(\theta, ka)$, we introduce a new integration variable

$$\theta'' = \theta' - \theta_0' = \theta' + \theta - 3\pi/2 \tag{93}$$

so that

$$K_\pi^{(+)}(\theta, ka) = \frac{1}{i\pi}\int_{-\infty}^{\infty}\int_{\theta-3\pi/2}^{\theta-\pi/2} e^{ikag_+(\theta'',t)}d\theta'' dt. \tag{94}$$

Expanding the exponent in a Taylor series about the second order stationary phase point at $(\theta'', t) = (0, 0)$ we find

$$g_+(\theta'', t) \approx (3\pi/2 - \theta)(1 + t^2/2) + \theta''^3/6 + \theta'' t^2/2. \tag{95}$$

The t-integral can be performed using the standard result [14]

$$\int_{-\infty}^{\infty} e^{ipt^2} dt = \sqrt{\frac{\pi}{p}}\, e^{i\pi/4}. \tag{96}$$

Thus

$$K_\pi^{(+)sp}(\theta,ka) \overset{ka\gg 1}{\approx} \frac{e^{ika(3\pi/2-\theta)}}{i\pi}\sqrt{\frac{2\pi}{ka}}e^{i\pi/4}\int_{\theta-3\pi/2}^{\theta-\pi/2}\frac{e^{ika\theta''^3/6}\ d\theta''}{\sqrt{\theta''+3\pi/2-\theta}} \quad \text{for } \pi/2<\theta\le\pi. \tag{97}$$

For $ka \gg 1$ the leading contribution to the remaining integral is of order $(ka)^{-1/3}$. This is the contribution due to the stationary phase point at $\theta''=0$:

$$\begin{aligned}\int_{\theta-3\pi/2}^{\theta-\pi/2}\frac{e^{ika\theta''^3/6}\ d\theta''}{\sqrt{\theta''+3\pi/2-\theta}} &\overset{ka\gg 1}{\approx} \frac{1}{\sqrt{3\pi/2-\theta}}\int_{-\infty}^{\infty}e^{ika\theta''^3/6}\ d\theta'' \\ &= \frac{2\pi}{\sqrt{3\pi/2-\theta}}\left(\frac{2}{ka}\right)^{1/3}Ai(0).\end{aligned} \tag{98}$$

Here we have used an integral representation of the Airy function $Ai(x)$ [14]. The constant $Ai(0)$ is approximately equal to 0.355. The effects of the finite integration limits will be considered more precisely (i.e. without the stationary phase approximation to the integrand) later in this Appendix. We have found that

$$K_\pi^{(+)sp}(\theta,ka) \overset{ka\gg 1}{\approx} \begin{cases} 0 & \text{for } 0\le\theta<\pi/2 \\ \left(\frac{8\pi}{ka}\right)^{1/2}\left(\frac{2}{ka}\right)^{1/3}e^{-i\pi/4}Ai(0)\frac{e^{ika(3\pi/2-\theta)}}{\sqrt{3\pi/2-\theta}} & \text{for } \pi/2<\theta\le\pi \end{cases} \tag{99}$$

A similar determination of the stationary phase point contribution to the integral $K_\pi^{(-)}(\theta,ka)$ is possible. Again a stationary phase point exists within the integration interval only when $\pi/2<\theta\le\pi$. It is located at $(\theta',t)=(\pi/2-\theta,0)$. The change of variable $\theta''=\theta'+\theta-\pi/2$ gives

$$K_\pi^{(-)}(\theta,ka)=\frac{1}{i\pi}\int_{-\infty}^{\infty}\int_{\theta-3\pi/2}^{\theta-\pi/2}e^{ikag_-(\theta'',t)}d\theta''dt. \tag{100}$$

Using (90), expanding about the stationary point at $(\theta'',t)=(0,0)$ yields

$$g_-(\theta'',t)\approx(\theta-\pi/2)(1+t^2/2)-\theta''^3/6-\theta''t^2/2. \tag{101}$$

Carrying out the t-integration as before, we find

$$K_\pi^{(-)sp}(\theta,ka) \overset{ka\gg 1}{\approx} \frac{e^{ika(\theta-\pi/2)}}{i\pi}\sqrt{\frac{2\pi}{ka}}e^{i\pi/4}\int_{\theta-3\pi/2}^{\theta-\pi/2}\frac{e^{-ika\theta''^3/6}\ d\theta''}{\sqrt{\theta-\pi/2-\theta''}} \quad \text{for } \pi/2<\theta\le\pi. \tag{102}$$

This time, however, the function multiplying the exponential in the integrand is not well-behaved near the stationary phase point $\theta''=0$ when $\theta\approx\pi/2$. Thus

$$\int_{\theta-3\pi/2}^{\theta-\pi/2}\frac{e^{-ika\theta''^3/6}\ d\theta''}{\sqrt{\theta-\pi/2-\theta''}} \overset{ka\gg 1}{\approx} \frac{2\pi}{\sqrt{\theta-\pi/2}}\left(\frac{2}{ka}\right)^{1/3}Ai(0) \tag{103}$$

provided $\theta \not\approx \pi/2$. Hence

$$K_\pi^{(-)sp}(\theta, ka) \overset{ka\gg 1, \theta \not\approx \pi/2}{\approx} \begin{cases} 0 & \text{for } 0 \le \theta < \pi/2 \\ \left(\frac{8\pi}{ka}\right)^{1/2} \left(\frac{2}{ka}\right)^{1/3} e^{-i\pi/4} Ai(0) \frac{e^{ika(\theta-\pi/2)}}{\sqrt{\theta-\pi/2}} & \text{for } \pi/2 < \theta \le \pi \end{cases} \tag{104}$$

and so from (87),(99) and (104) we deduce that

$$K_\pi^{sp}(\theta, ka) \overset{ka\gg 1, \cos\theta \not\approx 0}{\approx} U(|\theta| - \pi/2) \left(\frac{8\pi}{ka}\right)^{1/2} \left(\frac{2}{ka}\right)^{1/3} Ai(0) e^{-i\pi/4} \left(\frac{e^{ika(3\pi/2-|\theta|)}}{\sqrt{3\pi/2-|\theta|}} + \frac{e^{ika(|\theta|-\pi/2)}}{\sqrt{|\theta|-\pi/2}}\right). \tag{105}$$

Substituting into (85), we find the following contribution to $I_\pi(\theta, ka)$ arising from stationary phase considerations:

$$I_\pi^{sp}(\theta, ka) \overset{ka\gg 1, \cos\theta \not\approx 0}{\approx} U(|\theta| - \pi/2) \left(\frac{8\pi}{ka}\right)^{1/2} \left(\frac{2}{ka}\right)^{1/3} Ai(0) e^{-3i\pi/4} \left(\frac{e^{ika(3\pi/2-|\theta|)}}{(3\pi/2-|\theta|)^{3/2}} + \frac{e^{ika(|\theta|-\pi/2)}}{(|\theta|-\pi/2)^{3/2}}\right). \tag{106}$$

A.2 End-Point Contributions

Asymptotic series for the end-point contributions to the θ' integrals of (88) and (89) can be developed using successive integrations by parts:

$$\int_0^\pi e^{ikag_+(\theta',t)} d\theta' = \frac{e^{ikag_+(\pi,t)}}{ikag'_+(\pi,t)} \left\{1 + \frac{g''_+(\pi,t)}{ika(g'_+(\pi,t))^2} + 0\left(\frac{1}{ka}\right)^2\right\} - \frac{e^{ikag_+(0,t)}}{ikag'_+(0,t)} \left\{1 + \frac{g''_+(0,t)}{ika(g'_+(0,t))^2} + 0\left(\frac{1}{ka}\right)^2\right\} \tag{107}$$

$$\int_{-\pi}^0 e^{ikag_-(\theta',t)} d\theta' = \frac{e^{ikag_-(0,t)}}{ikag'_-(0,t)} \left\{1 + \frac{g''_-(0,t)}{ika(g'_-(0,t))^2} + 0\left(\frac{1}{ka}\right)^2\right\} - \frac{e^{ikag_-(-\pi,t)}}{ikag'_-(-\pi,t)} \left\{1 + \frac{g''_-(-\pi,t)}{ika(g'_-(-\pi,t))^2} + 0\left(\frac{1}{ka}\right)^2\right\}. \tag{108}$$

Here $g'_\pm$ and $g''_\pm$ respectively denote the first and second derivatives of $g_\pm$ with respect to θ'. Hence the end-point contributions to $K_\pi(\theta, ka)$ (denoted by $K_\pi^e(\theta, ka)$) are found to be

$$
\begin{aligned}
K_\pi^e(\theta,ka) &= \frac{e^{-ika\cos\theta}}{\pi ka}\left\{\int_{-\infty}^{\infty}\left(\frac{1}{\cosh t+\sin\theta}+\frac{1}{\cosh t-\sin\theta}\right)dt\right. \\
&\quad \left.+\frac{\cos\theta}{ika}\int_{-\infty}^{\infty}\left(\frac{1}{(\cosh t+\sin\theta)^3}+\frac{1}{(\cosh t-\sin\theta)^3}\right)dt+0\left(\frac{1}{ka}\right)^2\right\} \\
&- \frac{e^{ika\cos\theta}}{\pi ka}\left\{\int_{-\infty}^{\infty}\left(\frac{1}{\cosh t+\sin\theta}+\frac{1}{\cosh t-\sin\theta}\right)e^{i\pi ka\cosh t}dt\right. \\
&\quad -\frac{\cos\theta}{ika}\int_{-\infty}^{\infty}\left(\frac{1}{(\cosh t+\sin\theta)^3}+\frac{1}{(\cosh t-\sin\theta)^3}\right)e^{i\pi ka\cosh t}dt \\
&\quad \left.+0\left(\frac{1}{ka}\right)^2\right\}. \qquad (109)
\end{aligned}
$$

The first term is due to the discontinuity of the derivative of the integrand of $K_\pi(\theta,ka)$ at $\theta'=0$. The first t-integration can be performed by application of contour methods in the complex plane or by repeated use of the standard integral [15]

$$
\int_0^\infty \frac{dt}{\cosh t+\cos\alpha}=\frac{\alpha}{\sin\alpha} \qquad (0<\alpha<\pi). \qquad (110)
$$

We find

$$
\int_{-\infty}^{\infty}\left(\frac{1}{\cosh t+\sin\theta}+\frac{1}{\cosh t-\sin\theta}\right)dt=\frac{2\pi}{|\cos\theta|}. \qquad (111)
$$

Differentiating this result twice with respect to $\sin\theta$ gives

$$
\int_{-\infty}^{\infty}\left(\frac{1}{(\cosh t+\sin\theta)^3}+\frac{1}{(\cosh t-\sin\theta)^3}\right)dt=\frac{\pi}{|\cos\theta|}\frac{(3-2\cos^2\theta)}{\cos^4\theta}. \qquad (112)
$$

The second term of (109) is due to the truncation of the integrand at the end-points $\theta'=\pm\pi$. Provided $|\sin\theta|\not\approx 1$ the t-integrals can be evaluated for $ka\gg 1$ by the method of stationary phase. Expanding the integrands around the stationary phase point at $t=0$ in the usual way [14] we find

$$
\begin{aligned}
&\int_{-\infty}^{\infty}\left(\frac{1}{\cosh t+\sin\theta}+\frac{1}{\cosh t-\sin\theta}\right)e^{i\pi ka\cosh t}dt \overset{ka\gg 1,\cos\theta\not\approx 0}{=} \\
&\qquad \sqrt{\frac{8}{ka}}e^{i\pi ka}e^{i\pi/4}\frac{1}{\cos^2\theta}\left(1-\frac{i(8-3\cos^2\theta)}{8\pi ka\cos^2\theta}+0\left(\frac{1}{ka}\right)^2\right). \qquad (113)
\end{aligned}
$$

and

$$
\begin{aligned}
&\int_{-\infty}^{\infty}\left(\frac{1}{(\cosh t+\sin\theta)^3}+\frac{1}{(\cosh t-\sin\theta)^3}\right)e^{i\pi ka\cosh t}dt \overset{ka\gg 1,\cos\theta\not\approx 0}{=} \\
&\qquad \sqrt{\frac{8}{ka}}e^{i\pi ka}e^{i\pi/4}\frac{(4-3\cos^2\theta)}{\cos^6\theta}\left(1+0\left(\frac{1}{ka}\right)^2\right). \qquad (114)
\end{aligned}
$$

(As before, (114) can also be obtained by differentiating (113) twice with respect to $\sin\theta$.) Substituting (111),(112),(113) and (114) into (109) gives the end-point contribution to $K_\pi(\theta,ka)$:

$$K_\pi^e(\theta,ka) \overset{ka\gg 1,\cos\theta\neq 0}{=} \frac{2e^{-ika\cos\theta}}{ka|\cos\theta|}\left\{1+\frac{(3-2\cos^2\theta)}{2ika\cos^3\theta}+0\left(\frac{1}{ka}\right)^2\right\}$$
$$-\left(\frac{2}{ka}\right)^{3/2}\frac{e^{ika\cos\theta}e^{i\pi ka}e^{i\pi/4}}{\pi\cos^2\theta}$$
$$\cdot\left\{1-\frac{i(8-3\cos^2\theta)}{8\pi ka\cos^2\theta}+\frac{i(4-3\cos^2\theta)}{ka\cos^3\theta}+0\left(\frac{1}{ka}\right)^2\right\} \quad (115)$$

We now substitute this result into (85) to find the end-point contributions to $I_\pi(\theta,ka)$ (denoted $I_\pi^e(\theta,ka)$). After performing the necessary differentiations and much tedious algebra we find

$$I_\pi^e(\theta,ka) \overset{ka\gg 1,\cos\theta\neq 0}{=} 2|\cos\theta|e^{-ika\cos\theta}\left(1+\frac{i}{2ka\cos^3\theta}\right)$$
$$+I_\pi^t(\theta,ka)+0\left(\frac{1}{ka}\right)^2, \quad (116)$$

with

$$I_\pi^t(\theta,ka)=\left(\frac{2}{ka}\right)^{3/2}\frac{e^{3i\pi/4}e^{i\pi ka}e^{ika\cos\theta}}{\pi^2\cos^2\theta}. \quad (117)$$

We have included the first term on the right side of (85) and have used the asymptotic form of the Hankel function to arrive at this result. This is appropriate since that term originated from end-point contributions when integrating by parts. It is of interest to note that the term $I_\pi^t(\theta,ka)$, which is due to the truncation of the integration interval at $\theta'=\pm\pi$, can also be derived directly by considering $I_\infty - I_\pi$:

$$I_\infty(\theta,ka)-I_\pi(\theta,ka)=\left(\int_{-\infty}^{-\pi}+\int_{\pi}^{\infty}\right)\frac{H_1^{(1)}(ka\theta')}{\theta'}e^{-ika\cos(\theta'+\theta)}d\theta'. \quad (118)$$

Using the asymptotic form of the Hankel function we find

$$I_\infty(\theta,ka)-I_\pi(\theta,ka) \overset{ka\gg 1}{\approx} \sqrt{\frac{2}{\pi ka}}e^{-3i\pi/4}\int_\pi^\infty\frac{e^{ika\theta'}}{(\theta')^{3/2}}(e^{-ika\cos(\theta'+\theta)}+e^{-ika\cos(\theta'-\theta)})d\theta'$$
$$\overset{\cos\theta\neq 0}{=} \left(\frac{2}{ka}\right)^{3/2}\frac{e^{-i\pi/4}e^{i\pi ka}e^{ika\cos\theta}}{\pi^2\cos^2\theta}+0\left(\frac{1}{ka}\right)^{5/2}. \quad (119)$$

Thus

$$I_\pi(\theta,ka) \overset{ka\gg 1}{\approx} I_\infty(\theta,ka)+I_\pi^t(\theta,ka) \quad (120)$$

as required.

Finally, then, we add the stationary phase and end-point contributions to determine the asymptotic approximation to $I_\pi(\theta,ka)$:

$$I_\pi(\theta,ka) \overset{ka\gg 1}{\approx} I_\pi^{sp}(\theta,ka)+I_\pi^e(\theta,ka), \quad (121)$$

where I_π^{sp} and I_π^e are given by (106) and (116) respectively.

B Asymptotic ($ka \gg 1$) Analysis of $\psi^c(s,0)$

Our starting point is the exact expression (32):

$$\psi^c(s,0) = \frac{-k}{2\pi a} \sum_{l=-\infty}^{\infty} f(l,ka) e^{il\theta} \tag{122}$$

with

$$\theta = s/a \tag{123}$$

and

$$f(l,ka) = \frac{H_l^{(1)\prime}(ka)}{H_l^{(1)}(ka)}. \tag{124}$$

An asymptotic investigation is possible by means of a Watson transformation [11]. Using this technique the infinite sum is converted to a contour integral in the complex plane (see Fig.11):

$$\sum_{l=-\infty}^{\infty} f(l,ka) e^{il\theta} = \frac{i}{2} \int_{C_+ + C_-} \frac{e^{i\nu(\theta+\pi)}}{\sin \nu\pi} f(\nu,ka) d\nu. \tag{125}$$

This step is easily checked by evaluating the residues of the (simple) poles of $\sin \nu\pi$ which lie on the real axis. The assumption has been made that $f(\nu,ka)$ has no poles lying within the contour $C_+ + C_-$. By choosing the positive constant σ to be arbitrarily small this is indeed the case — $H_\nu^{(1)}(ka) = 0$ has no solution for real ν. Since [14]

$$H_\nu^{(1)}(ka) = e^{-i\nu\pi} H_{-\nu}^{(1)}(ka) \tag{126}$$

$$H_\nu^{(1)\prime}(ka) = e^{-i\nu\pi} H_{-\nu}^{(1)\prime}(ka), \tag{127}$$

we deduce that

$$f(\nu,ka) = f(-\nu,ka). \tag{128}$$

Hence

$$\psi^c(s,0) = \frac{-ik}{2\pi a} \int_{C_+} \frac{\cos \nu(\theta+\pi)}{\sin \nu\pi} f(\nu,ka) d\nu. \tag{129}$$

Following the analogous treatment of the field scattered by a perfectly conducting cylinder due to plane wave incidence [11] we choose to write

$$\cos \nu(\theta+\pi) = -ie^{-i\nu\theta} \sin \nu\pi + e^{i\nu\pi} \cos \nu\theta \tag{130}$$

and examine the contributions of these terms separately. It remains to be seen whether similar physical interpretations can be given to these contributions.

The integrand of (129) due to the first term on the right side of (130) has no poles lying on the real axis. Thus the integration contour may be taken to be that axis:

$$\psi^{c(1)}(s,0) = \frac{-k}{2\pi a} \int_{-\infty}^{\infty} e^{-i\nu\theta} f(\nu,ka) d\nu. \tag{131}$$

As far as the author is aware the Fourier transform of $f(\nu, ka)$ is not known. To proceed further we thus revert to a uniform asymptotic expansion of $f(\nu, ka)$. Applying known uniform asymptotic expansions of both $H_\nu^{(1)\prime}(ka)$ and $H_\nu^{(1)}(ka)$ [16], it follows that

$$f(\nu, ka) = \frac{H_\nu^{(1)\prime}(ka)}{H_\nu^{(1)}(ka)} \overset{ka \gg 1, |\nu| \sim ka}{\approx} -\frac{\gamma(\nu, ka)}{ka} + \frac{ka}{2(\nu^2 - (ka)^2)}, \tag{132}$$

where $\gamma(\nu, ka)$ is defined in (19). The error is of order $0(|\nu|)^{-2}$ or $0(ka)^{-2}$. Inserting the leading order term into (131) we obtain a contribution to $\psi^{c(1)}(s, 0)$ of

$$\frac{1}{2\pi a^2} \int_{-\infty}^{\infty} e^{-i\nu s/a} \gamma(\nu, ka) d\nu = \frac{-ik}{2} \frac{H_1^{(1)}(ks)}{s}, \tag{133}$$

where the integral has been evaluated using (23) and (24). All dependence on ka has disappeared and we have recovered $\psi^p(s, 0)$. The next-to-leading order term of (132) contributes

$$\frac{-k^2}{4\pi} \int_{-\infty}^{\infty} \frac{e^{-i\nu s/a}}{(\nu^2 - (ka)^2)} d\nu. \tag{134}$$

To evaluate this integral we need to know how to treat the poles at $\nu = \pm ka$. This problem is resolved by considering their origin. They have arisen because we have used the approximation (132). However a closer examination of the zeroes $\nu_n (n = 1, 2, \ldots)$ of $H_\nu^{(1)}(ka)$ [17] reveals that (for $Re(\nu) > 0$) they lie approximately along a line oriented at 60° to the positive real axis:

$$\nu_n = ka + \alpha_n e^{i\pi/3} \left(\frac{ka}{2}\right)^{1/3} + 0(ka)^{-1/3}. \tag{135}$$

The real constants α_n are related to zeroes of the Airy function:

$$Ai(-\alpha_n) = 0. \tag{136}$$

As the α_n are positive, $Im(\nu_n) > 0$. Thus the pole of (134) at $\nu = ka$ should be taken to lie just above the real axis. Also, in view of (128), the pole at $\nu = -ka$ is taken to lie just below the real axis. Evaluation of (134) then follows by straightforward application of Cauchy's integral formula:

$$\frac{-k^2}{4\pi} \int_{-\infty}^{\infty} \frac{e^{-i\nu s/a}}{(\nu^2 - (ka)^2)} d\nu = \frac{-ik}{4a} e^{ik|s|}. \tag{137}$$

From (131), (132), (133) and (137), then, it follows that

$$\psi^{c(1)}(s, 0) = \psi^p(s, 0) - \frac{ik}{4a} e^{ik|s|} + k^2 . 0(ka)^{-2}. \tag{138}$$

The second term represents a first order curvature correction to $\psi^p(s, 0)$.

We now consider the contribution of the second term of (130):

$$\psi^{c(2)}(s,0) = \frac{-k}{\pi a}\int_{C_+} \frac{e^{2i\nu\pi}\cos\nu\theta}{(1-e^{2i\nu\pi})} f(\nu,ka)d\nu. \tag{139}$$

The integrand has simple poles at the zeroes of $\sin\nu\pi$ and at $\nu = \pm\nu_n$, where $H^{(1)}_{\nu_n}(ka) = 0$. Referring to Fig.12, we see that

$$\int_C \frac{e^{2i\nu\pi}\cos\nu\theta}{(1-e^{2i\nu\pi})} f(\nu,ka)d\nu = 0, \tag{140}$$

where the contour C is given by $C = C_+ + C_1 + C_2 + C_3$. Consider the contributions of the arcs at infinity (C_1 and C_3). From (132),

$$f(\nu,ka) \overset{ka\gg 1,|\nu|\to\infty}{\sim} \frac{-|\nu|}{ka}. \tag{141}$$

Since $Im(\nu) > 0$ and $|\theta| \le \pi$, this behaviour is swamped by a decaying exponential due to the rest of the integrand. It is therefore clear that the integrals along C_1 and C_3 vanish. Thus

$$\psi^{c(2)}(s,0) = \frac{k}{\pi a}\int_{C_2} \frac{e^{2i\nu\pi}\cos\nu\theta}{(1-e^{2i\nu\pi})} f(\nu,ka)d\nu. \tag{142}$$

Applying Cauchy's integral formula once again we find

$$\psi^{c(2)}(s,0) = \frac{-2ik}{a}\sum_{n=1}^{\infty} \frac{e^{2i\nu_n\pi}\cos\nu_n\theta}{(1-e^{2i\nu_n\pi})} \frac{H^{(1)\prime}_{\nu_n}(ka)}{\frac{\partial}{\partial\nu}H^{(1)}_{\nu}(ka)|_{\nu=\nu_n}}, \tag{143}$$

where the sum is over the residues of the poles at ν_n. A Wronskian relation for Hankel functions [17] enables us to write

$$\frac{H^{(1)\prime}_{\nu_n}(ka)}{\frac{\partial}{\partial\nu}H^{(1)}_{\nu}(ka)|_{\nu=\nu_n}} = \frac{4i}{\pi ka H^{(2)}_{\nu_n}(ka)\frac{\partial}{\partial\nu}H^{(1)}_{\nu}(ka)|_{\nu=\nu_n}}. \tag{144}$$

James [14] gives the following useful asymptotic forms for Hankel functions:

$$H^{(1)}_{\nu}(ka) \overset{\nu\approx ka\gg 1}{\approx} 2\left(\frac{2}{ka}\right)^{1/3} e^{-i\pi/3} Ai\left\{(\nu-ka)\left(\frac{2}{ka}\right)^{1/3} e^{2i\pi/3}\right\} \tag{145}$$

$$H^{(2)}_{\nu}(ka) \overset{\nu\approx ka\gg 1}{\approx} 2\left(\frac{2}{ka}\right)^{1/3} e^{i\pi/3} Ai\left\{(\nu-ka)\left(\frac{2}{ka}\right)^{1/3} e^{-2i\pi/3}\right\}. \tag{146}$$

From (145) we deduce

$$\frac{\partial}{\partial\nu}H^{(1)}_{\nu}(ka) \overset{\nu\approx ka\gg 1}{\approx} 2\left(\frac{2}{ka}\right)^{2/3} e^{i\pi/3} Ai'\left\{(\nu-ka)\left(\frac{2}{ka}\right)^{1/3} e^{2i\pi/3}\right\}. \tag{147}$$

Since, for large ka, $\nu_n \approx ka$ and

$$(\nu_n - ka)\left(\frac{2}{ka}\right)^{1/3} \approx \alpha_n e^{i\pi/3} \tag{148}$$

(see (135)), we find

$$H_{\nu_n}^{(2)}(ka) \overset{ka\gg 1}{\approx} 2\left(\frac{2}{ka}\right)^{1/3} e^{i\pi/3} Ai(\alpha_n e^{-i\pi/3}) \tag{149}$$

$$\frac{\partial}{\partial \nu} H_{\nu}^{(1)}(ka)|_{\nu=\nu_n} \overset{ka\gg 1}{\approx} 2\left(\frac{2}{ka}\right)^{2/3} e^{i\pi/3} Ai'(-\alpha_n). \tag{150}$$

Thus, from (144),

$$\frac{H_{\nu_n}^{(1)\prime}(ka)}{\frac{\partial}{\partial \nu} H_{\nu}^{(1)}(ka)|_{\nu=\nu_n}} \overset{ka\gg 1}{\approx} \frac{i}{2\pi e^{2i\pi/3} Ai(\alpha_n e^{-i\pi/3}) Ai'(-\alpha_n)}. \tag{151}$$

Invoking the Wronskian relation [18]

$$e^{i\pi/3} Ai'(xe^{i\pi/3}) Ai(-x) + Ai(xe^{i\pi/3}) Ai'(-x) = \frac{-ie^{-i\pi/3}}{2\pi} \tag{152}$$

and (136) this becomes

$$\frac{H_{\nu_n}^{(1)\prime}(ka)}{\frac{\partial}{\partial \nu} H_{\nu}^{(1)}(ka)|_{\nu=\nu_n}} \overset{ka\gg 1}{\approx} -1. \tag{153}$$

Substituting into (143),

$$\psi^{c(2)}(s,0) \overset{ka\gg 1}{\approx} \frac{2ik}{a} \sum_{n=1}^{\infty} \frac{e^{2i\nu_n \pi} \cos \nu_n \theta}{(1 - e^{2i\nu_n \pi})}. \tag{154}$$

Since $Im(\nu_n) > 0$ this may be rewritten as

$$\psi^{c(2)}(s,0) \overset{ka\gg 1}{\approx} \frac{ik}{a} \sum_{n=1}^{\infty} \sum_{m=1}^{\infty} (e^{i\nu_n(2m\pi+\theta)} + e^{i\nu_n(2m\pi-\theta)}). \tag{155}$$

This form clearly suggests a creeping wave interpretation. Recalling that $\nu_n \approx ka$ for large ka we see that when $\theta = 0$ the phase factors correspond to waves which have completely encircled the cylinder m times in both a clockwise and anticlockwise sense.

Finally, then, from (138) and (155) it follows that

$$\begin{aligned} \psi^{c}(s,0) &= \psi^{c(1)}(s,0) + \psi^{c(2)}(s,0) \\ &\overset{ka\gg 1}{\approx} \psi^{p}(s,0) - \frac{ik}{4a} e^{ik|s|} \\ &\quad + \frac{ik}{a} \sum_{n=1}^{\infty} \sum_{m=1}^{\infty} (e^{i\nu_n(2m\pi+\theta)} + e^{i\nu_n(2m\pi-\theta)}) \end{aligned} \tag{156}$$

C Analysis of the Integral $M_\pi(\theta, ka)$

The integral $M_\pi(\theta, ka)$ (Eq.(68)) occurs in the IDBO treatment of scattering by a conducting circular cylinder. Exact analytic evaluation appears not to be possible. Here we give an approximate evaluation valid when $ka \gg 1$. We write

$$M_\pi(\theta, ka) = M_\pi^{(+)}(\theta, ka) + M_\pi^{(-)}(\theta, ka), \tag{157}$$

with

$$M_\pi^{(+)}(\theta, ka) = \int_0^\pi e^{ka h_+(\theta')} d\theta' \tag{158}$$

$$M_\pi^{(-)}(\theta, ka) = \int_{-\pi}^0 e^{ka h_-(\theta')} d\theta' \tag{159}$$

$$h_\pm(\theta') = \pm i \left(\frac{\nu_0}{ka}\right) \theta' - i\cos(\theta' + \theta). \tag{160}$$

Since $M_\pi(\theta, ka) = M_\pi(-\theta, ka)$ we confine the analysis to the case $0 \leq \theta \leq \pi$. Saddle point and end-point contributions are now considered in turn.

C.1 Saddle Point Contributions

Consider first the integral $M_\pi^{(+)}(\theta, ka)$. For a saddle point at $\theta' = \theta_0'$ (possibly complex) we have

$$h_+'(\theta_0') = i\left(\frac{\nu_0}{ka}\right) + i\sin(\theta_0' + \theta) = 0. \tag{161}$$

Since $\nu_0 \approx ka$ for $ka \gg 1$ (see (66)) solutions to this equation occur in closely spaced pairs in the complex θ' plane. It is not permissible to treat them separately. Instead, following arguments similar to Jones [19], we expand about their mid-point $\theta' = \theta_1'$, defined by

$$h_+''(\theta_1') = i\cos(\theta_1' + \theta) = 0. \tag{162}$$

For $0 \leq \theta < \pi/2$ this equation has no solution in the integration interval $0 < \theta' < \pi$ close to a saddle point pair. For $\pi/2 < \theta \leq \pi$, however, there is an appropriate solution at $\theta_1' = 3\pi/2 - \theta$. The associated saddle points $P_\pm$ are at

$$\theta' \approx \theta_1' \pm \sqrt{\alpha_0}\left(\frac{2}{ka}\right)^{1/3} e^{2i\pi/3} \tag{163}$$

and the steepest descents path passes through $P_\pm$ with slopes $\tan^{-1}(\pi/6 \mp \pi/4)$. Thus, for $\pi/2 < \theta \leq \pi$,

$$M_\pi^{(+)}(\theta, ka) \overset{ka \gg 1}{\approx} \int_C e^{ka\{h_+(\theta_1') + t h_+'(\theta_1') + (t^3/6) h_+'''(\theta_1')\}} dt \tag{164}$$

where $t = \theta' - \theta_1'$ and the contour $C = C_t^- + C_\infty^- + C_1 + C_\infty^+ + C_t^+$. (See Fig.13.) The contributions from the arcs at infinity (C_∞^- and C_∞^+) vanish. The contributions from

C_t^- and C_t^+ represent the effects of the truncation of the integrand of $M_\pi^{(+)}(\theta, ka)$ at $\theta' = \pm\pi$ and will be considered more precisely (i.e. without the saddle point approximation to the integrand) later in this Appendix. Deforming the steepest descents contour C_1 and using the substitution

$$z = \left(\frac{ka}{2}\right)^{1/3} e^{-i\pi/2}\ t \tag{165}$$

yields the saddle point contribution $M_\pi^{(+)sp}(\theta, ka)$ to $M_\pi^{(+)}(\theta, ka)$:

$$M_\pi^{(+)sp}(\theta, ka) \overset{ka\gg 1}{\approx} U(\theta - \pi/2)(-i)\left(\frac{2}{ka}\right)^{1/3} e^{i\nu_0(3\pi/2-\theta)} \cdot\left\{\int_{\infty e^{-i\pi/3}}^{0} + \int_0^{\infty e^{i\pi/3}}\right\} e^{(z^3/3+\alpha_0 e^{-2i\pi/3}z)}dz. \tag{166}$$

The remaining integrals furnish a familiar representation of the Airy function [14]. We find (for $0 \le \theta \le \pi$)

$$M_\pi^{(+)sp}(\theta, ka) \overset{ka\gg 1}{\approx} U(\theta - \pi/2)\ 2\pi\left(\frac{2}{ka}\right)^{1/3} Ai(\alpha_0 e^{i\pi/3}) e^{i\nu_0(3\pi/2-\theta)}. \tag{167}$$

An analogous treatment of the saddle point contributions to $M_\pi^{(-}(\theta, ka)$ is possible. The result (again for $0 \le \theta \le \pi$) is given below:

$$M_\pi^{(-)sp}(\theta, ka) \overset{ka\gg 1}{\approx} U(\theta - \pi/2)\ 2\pi\left(\frac{2}{ka}\right)^{1/3} Ai(\alpha_0 e^{i\pi/3}) e^{i\nu_0(\theta-\pi/2)}. \tag{168}$$

C.2 End-Point Contributions

Asymptotic series for the end-point contributions to the integral $M_\tau(\theta, ka)$ can be developed in the usual way (see Appendix A). We find

$$M_\pi^e(\theta, ka) \overset{ka\gg 1}{\approx} \frac{2i\nu_0}{(\nu_0^2 - (ka)^2\sin^2\theta)}(e^{-ika\cos\theta} - e^{i\nu_0\pi}e^{ika\cos\theta}). \tag{169}$$

The first term arises from the discontinuity in the derivative of the integrand at $\theta' = 0$ while the second term is due to the truncation of the integrand at the end-points $\theta' = \pm\pi$.

Finally, then, we add the saddle point and end-point contributions to determine the asymptotic approximation to $M_\tau(\theta, ka)$:

$$M_\tau(\theta, ka) \overset{ka\gg 1}{\approx} M_\pi^{(+)sp}(\theta, ka) + M_\pi^{(-)sp}(\theta, ka) + M_\tau^e(\theta, ka), \tag{170}$$

where $M_\pi^{(+)sp}$, $M_\pi^{(-)sp}$ and M_τ^e are given by (167), (168) and (169) respectively.

D Contribution of $\psi^{c(2)}(s,0)$ to the Cylinder Current

Here we compute the DBO contributions to the cylinder current due to creeping waves which traverse more than half the cylinder circumference. Such waves are accounted for by the term $\psi^{c(2)}(s,0)$ of (57). We begin with the form (154):

$$\psi^{c(2)}(s,0) \overset{ka\gg 1}{\approx} \frac{2ik}{a} \sum_{n=1}^{\infty} \frac{e^{2i\nu_n\pi}\cos\nu_n\theta}{(1-e^{2i\nu_n\pi})} \tag{171}$$

From (38) we deduce that this generates a contribution $j^{(2)}(\theta)$ to the current:

$$j^{(2)}(\theta) \overset{ka\gg 1}{\approx} ik \sum_{n=1}^{\infty} \frac{e^{2i\nu_n\pi}}{(1-e^{2i\nu_n\pi})} N_\pi(\theta,ka), \tag{172}$$

where

$$N_\pi(\theta,ka) = \int_{-\pi}^{\pi} (e^{i\nu_n\theta'} + e^{-i\nu_n\theta'}) e^{-ika\cos(\theta'+\theta)} d\theta'. \tag{173}$$

This integral bears many similarities to the integral $M_\pi(\theta,ka)$ analysed in Appendix C. An analogous asymptotic treatment is possible. We find

$$N_\pi(\theta,ka) \overset{ka\gg 1}{\approx} N_\pi^{sp}(\theta,ka) + N_\pi^{t}(\theta,ka), \tag{174}$$

where the end-point and saddle point contributions are given respectively by

$$N_\pi^{t}(\theta,ka) \overset{ka\gg 1}{\approx} \frac{4\nu_n \sin\nu_n\pi}{(\nu_n^2-(ka\sin\theta)^2)} e^{ika\cos\theta} \tag{175}$$

and

$$N_\pi^{sp}(\theta,ka) \overset{ka\gg 1}{\approx} \begin{cases} 2\pi\left(\frac{2}{ka}\right)^{1/3} Ai(\alpha_n e^{i\pi/3})(e^{-i\nu_n(\theta+\pi/2)} + e^{i\nu_n(\theta-\pi/2)}) & \text{for } 0 \le |\theta| \lesssim \pi/2 \\ 2\pi\left(\frac{2}{ka}\right)^{1/3} Ai(\alpha_n e^{i\pi/3})(e^{i\nu_n(|\theta|-\pi/2)} + e^{i\nu_n(3\pi/2-|\theta|)}) & \text{for } \pi/2 \lesssim |\theta| \le \pi \end{cases} \tag{176}$$

The end-point term arises, as usual, because of the truncation of the integration interval at $\theta' = \pm\pi$ and contributes

$$-2ke^{ika\cos\theta} \sum_{n=1}^{\infty} \frac{\nu_n e^{i\nu_n\pi}}{(\nu_n^2-(ka\sin\theta)^2)} \tag{177}$$

to the current. As expected the magnitude of this contribution is negligibly small. The contributions of the saddle point terms (176) to the cylinder current are

$$\begin{cases} -ike^{i\pi/6}\left(\frac{2}{ka}\right)^{1/3} \sum_{n=1}^{\infty} \frac{(e^{i\nu_n(3\pi/2-\theta)}+e^{i\nu_n(3\pi/2+\theta)})}{Ai'(-\alpha_n)(1-e^{2i\nu_n\pi})} & \text{for } 0 \le |\theta| \lesssim \pi/2 \\ -ike^{i\pi/6}\left(\frac{2}{ka}\right)^{1/3} \sum_{n=1}^{\infty} \frac{(e^{i\nu_n(3\pi/2+|\theta|)}+e^{i\nu_n(7\pi/2-|\theta|)})}{Ai'(-\alpha_n)(1-e^{2i\nu_n\pi})} & \text{for } \pi/2 \lesssim |\theta| \le \pi, \end{cases} \tag{178}$$

where we have used the relation

$$Ai(\alpha_n e^{i\pi/3})Ai'(-\alpha_n) = \frac{e^{-5i\pi/6}}{2\pi}. \tag{179}$$

(This follows from (152) using $Ai(-\alpha_n) = 0$.) Comparing with the asymptotic form (49) of the exact current we see that we have generated the correct creeping wave series in the illuminated region. Furthermore, by using the expansion

$$(1 - e^{2i\nu_n\pi})^{-1} = \sum_{m=0}^{\infty} e^{2i\nu_n m\pi} \tag{180}$$

(valid since $Im(\nu_n) > 0$) it is straightforward to confirm that the precise form of all higher order (i.e. $m > 0$) creeping wave contributions to the current on the shadowed side of the cylinder has been reproduced in (178). These terms represent waves which have completely encircled the cylinder at least once.

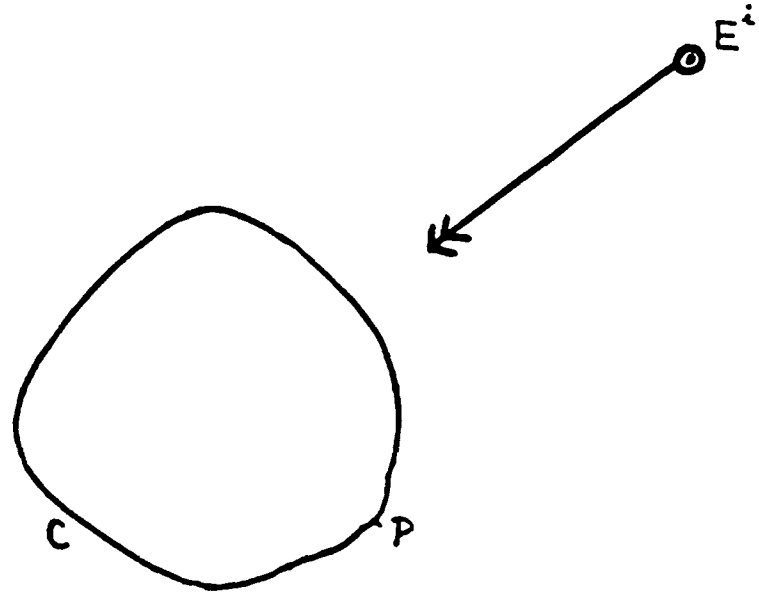

Fig.1. Electromagnetic scattering problem: infinite cylinder illuminated by plane wave.

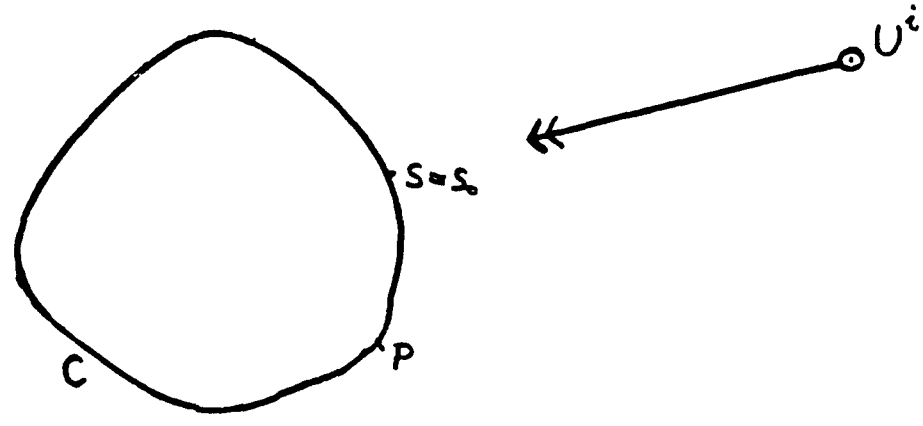

Fig.2. DBO problem: infinite cylinder illuminated by fictitious source.

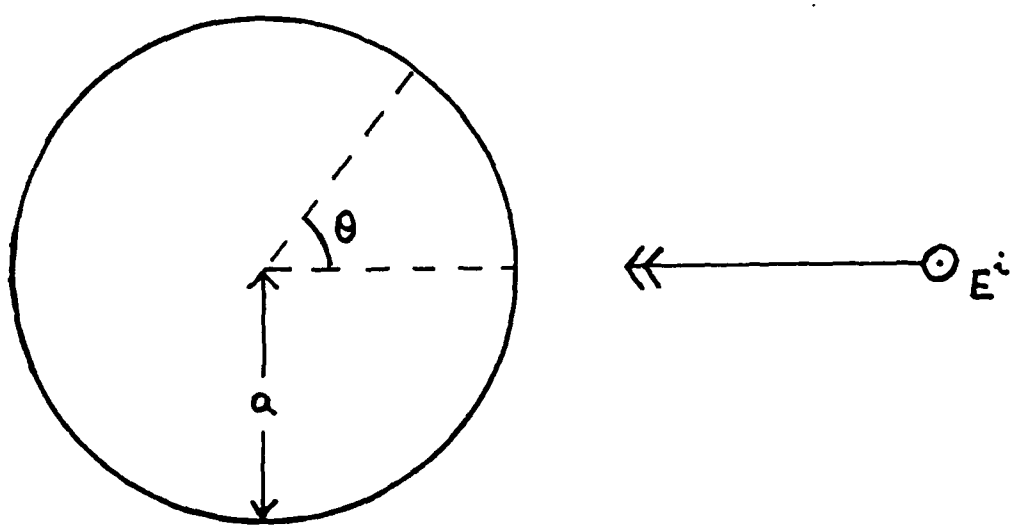

Fig.3. Plane wave scattering by an infinite circular cylinder.

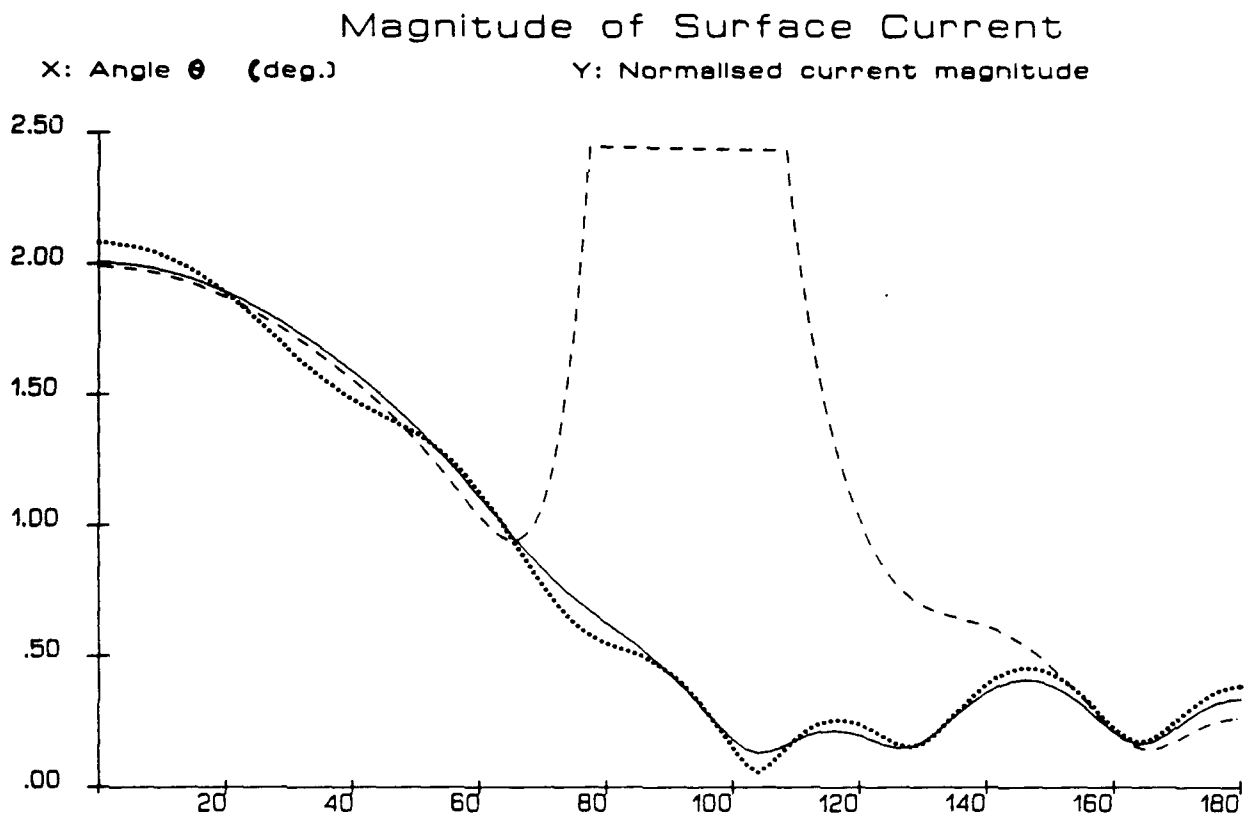

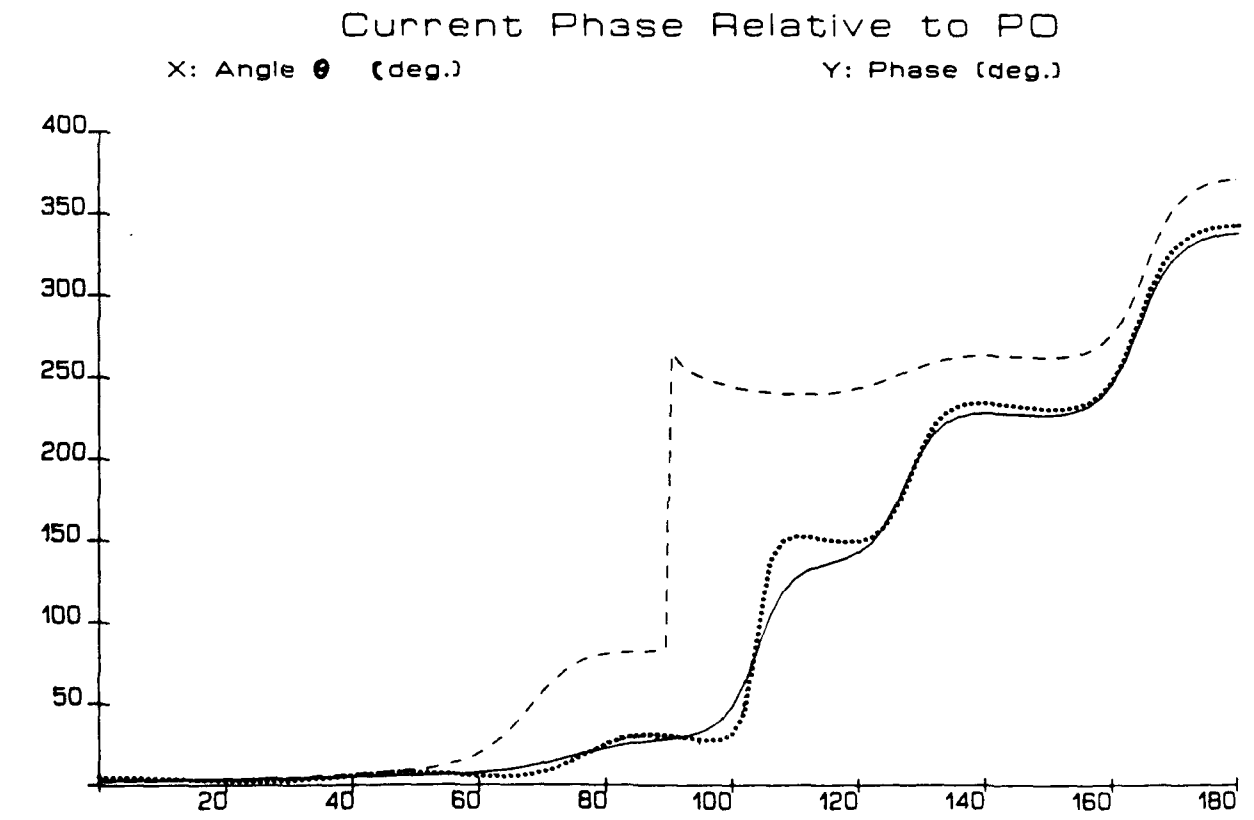

Fig.4(a). ADBO predictions of circular cylinder current ($ka = 5$).

—— using I_π (eq.(41))

..... using I_∞

- - - - using analytic approximation to I_π (eq.(48))

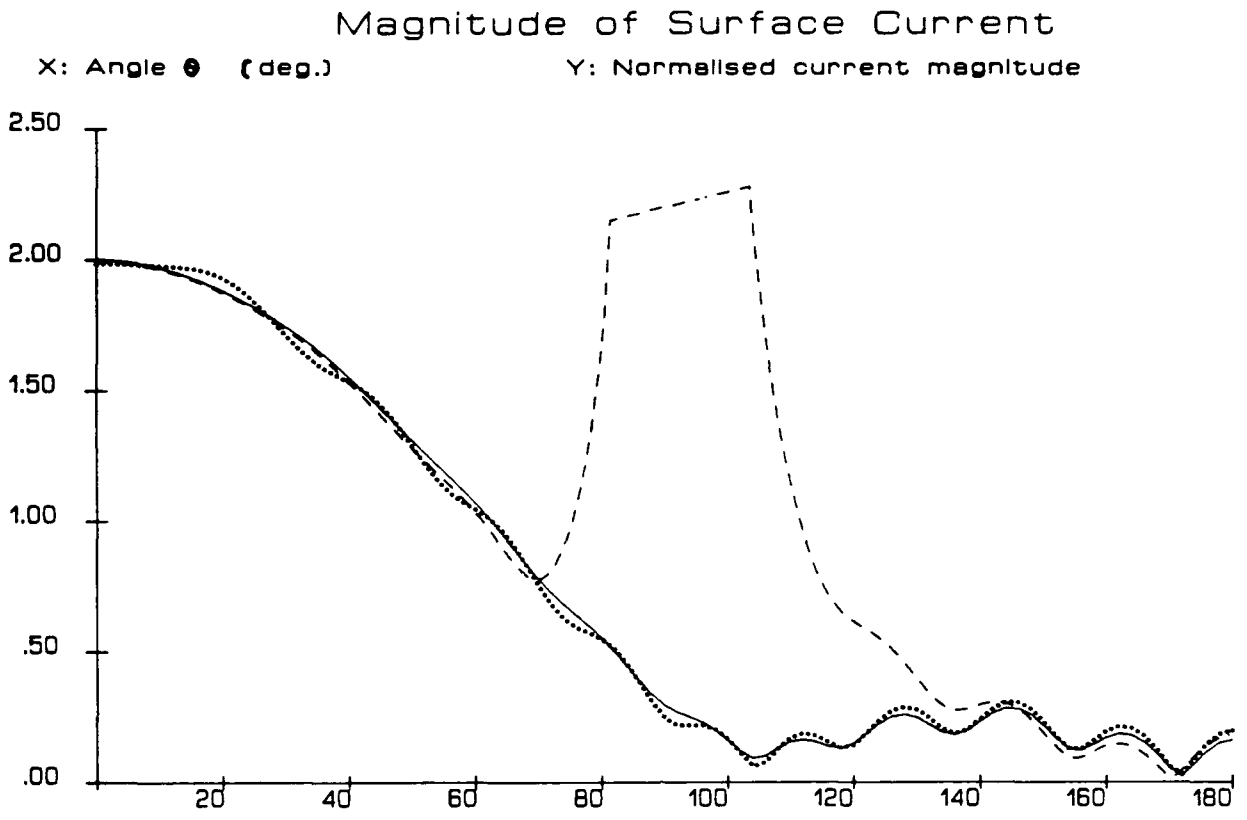

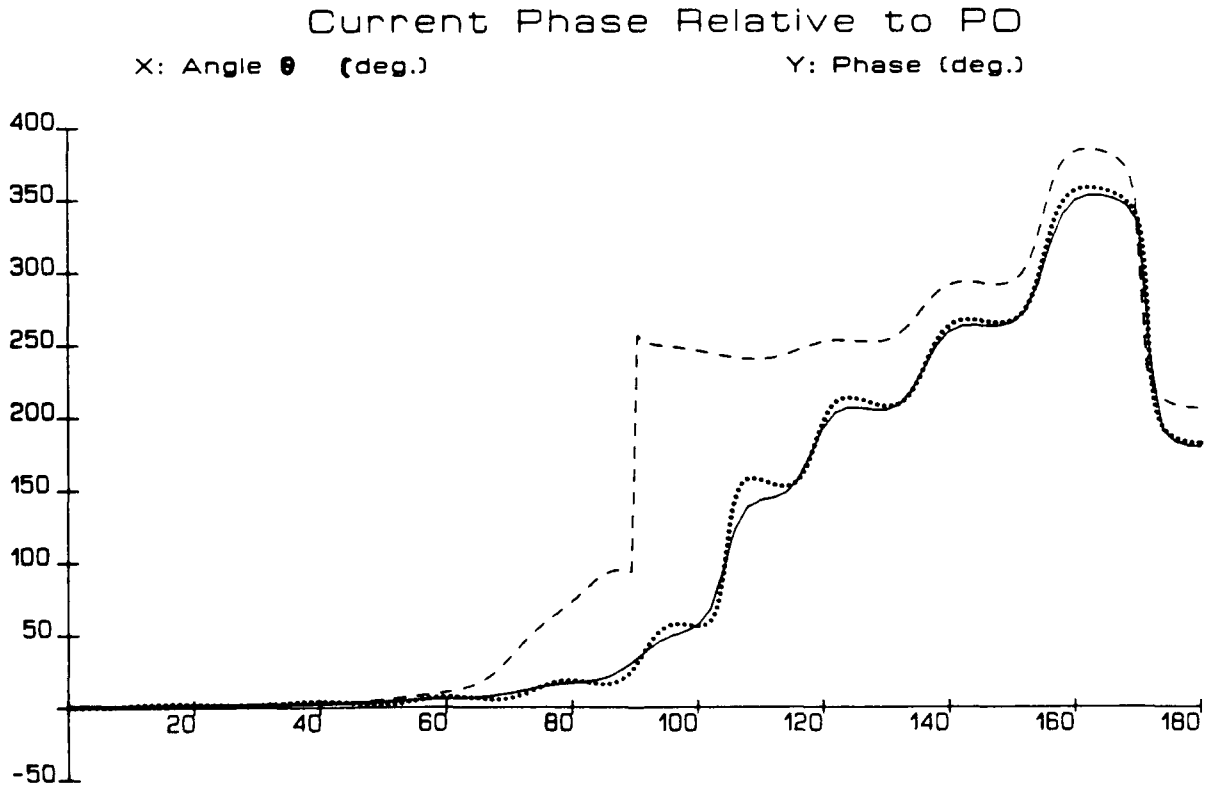

Fig.4(b). ADBO predictions of circular cylinder current ($ka = 10$).

—— using I_π (eq.(41))

..... using I_∞

- - - - using analytic approximation to I_π (eq.(48))

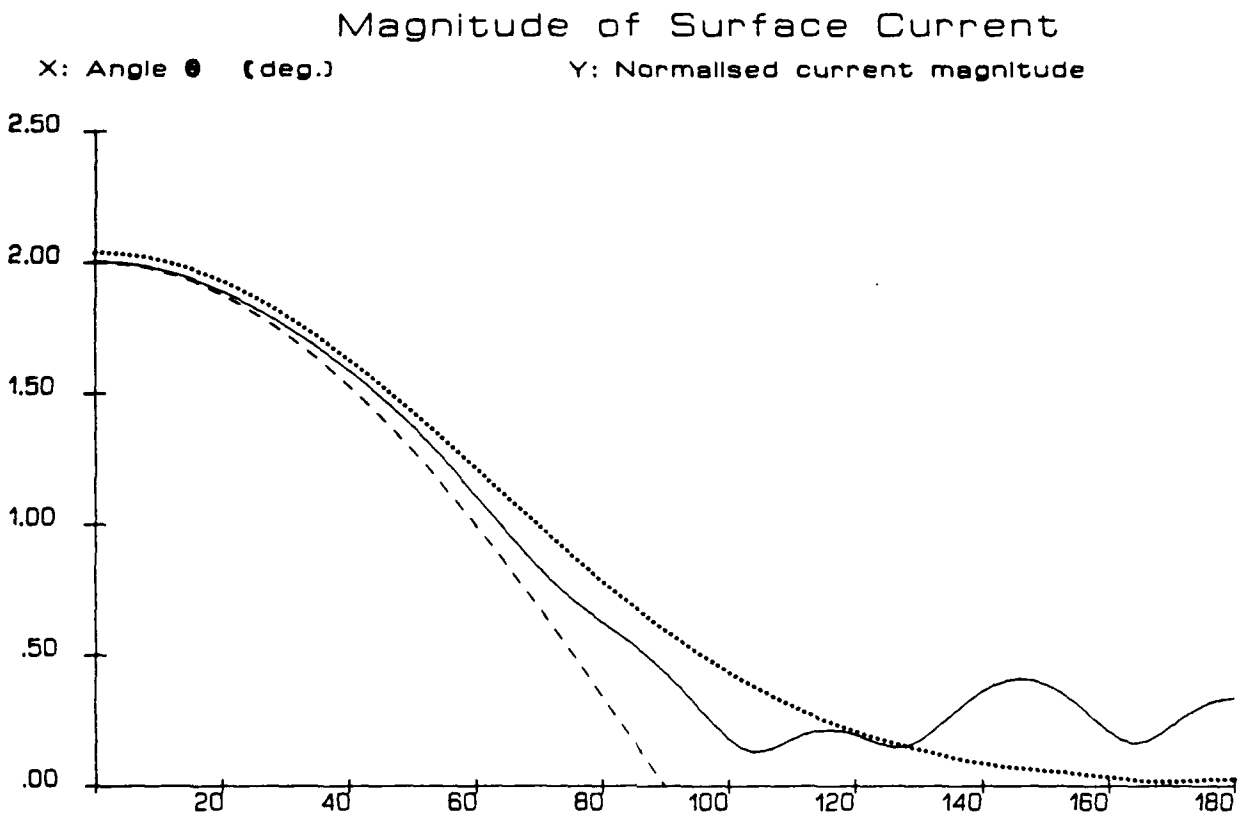

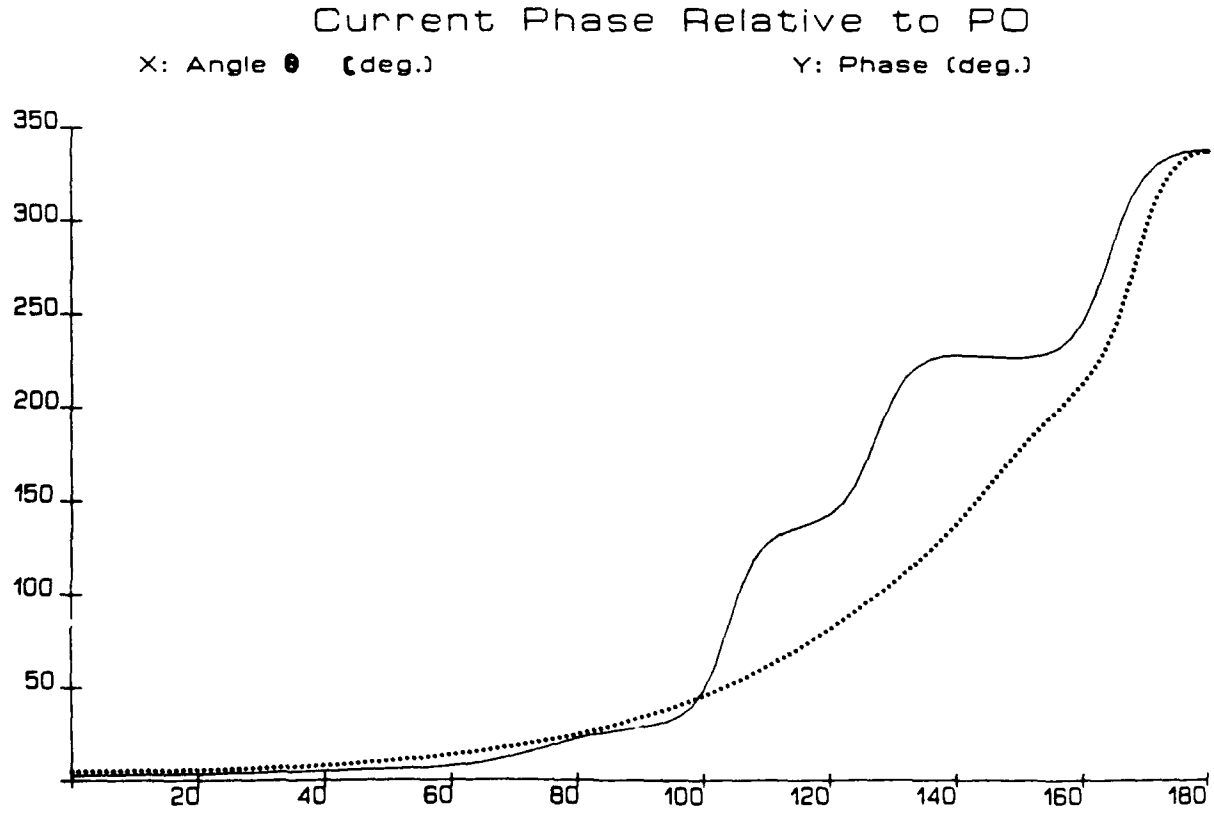

Fig.5(a). Circular cylinder surface current ($ka = 5$).

——— ADBO solution (using I_π)

. . . . . Exact solution

- - - - PO solution

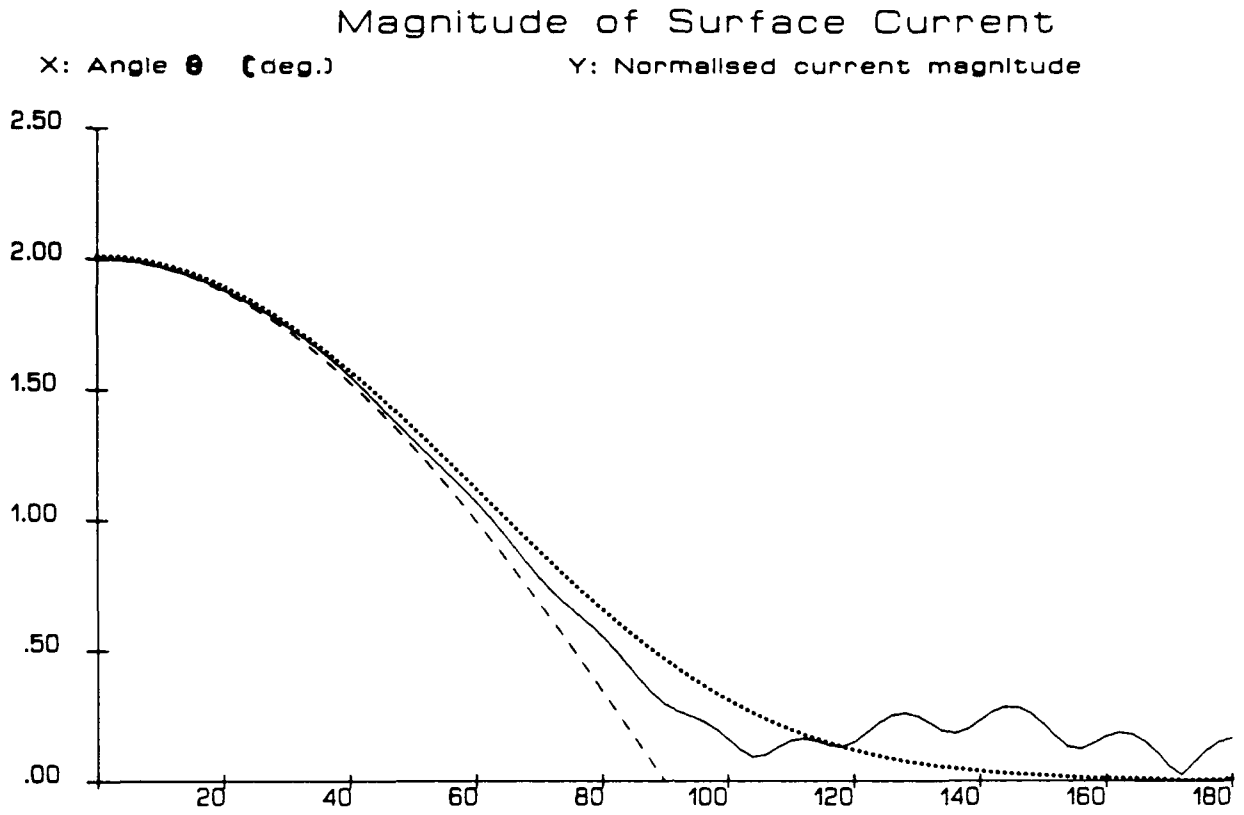

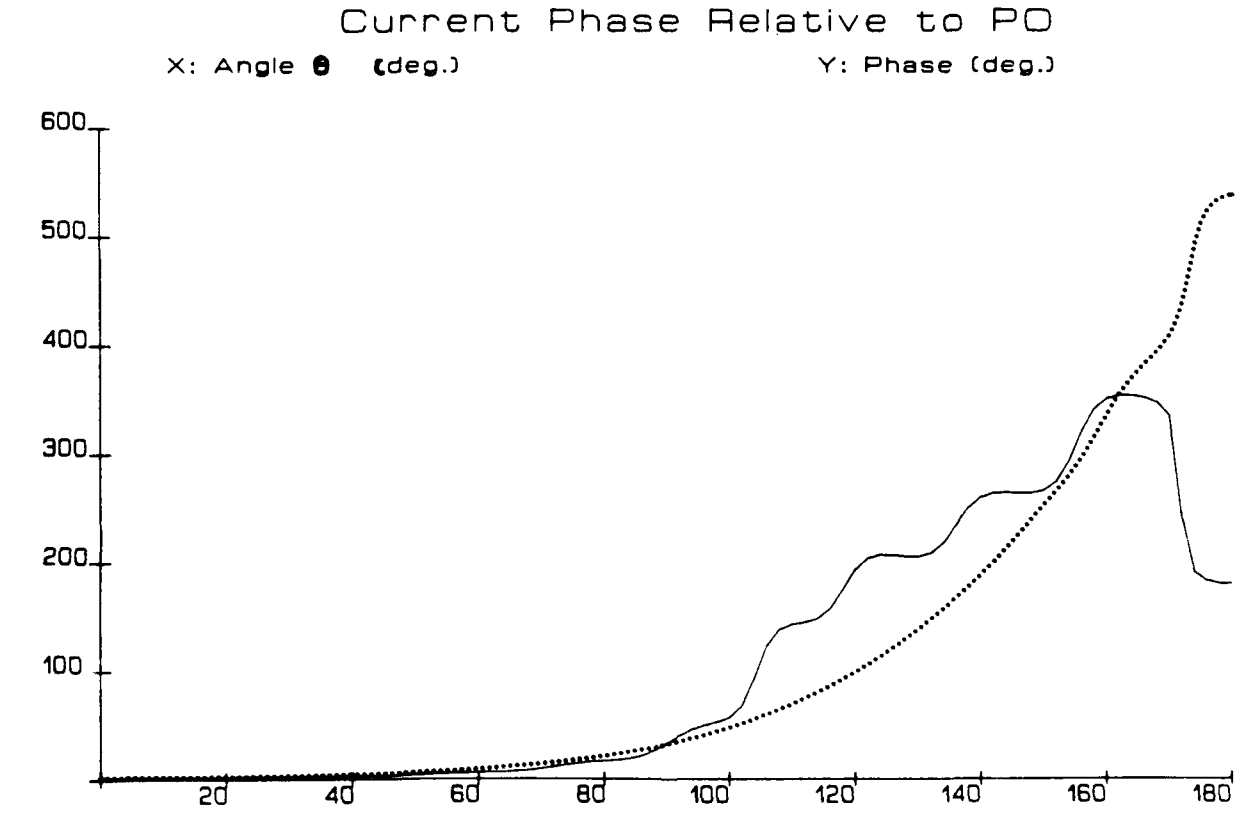

Fig.5(b). Circular cylinder surface current ($ka = 10$).

—— ADBO solution (using I_π)

..... Exact solution

- - - - PO solution

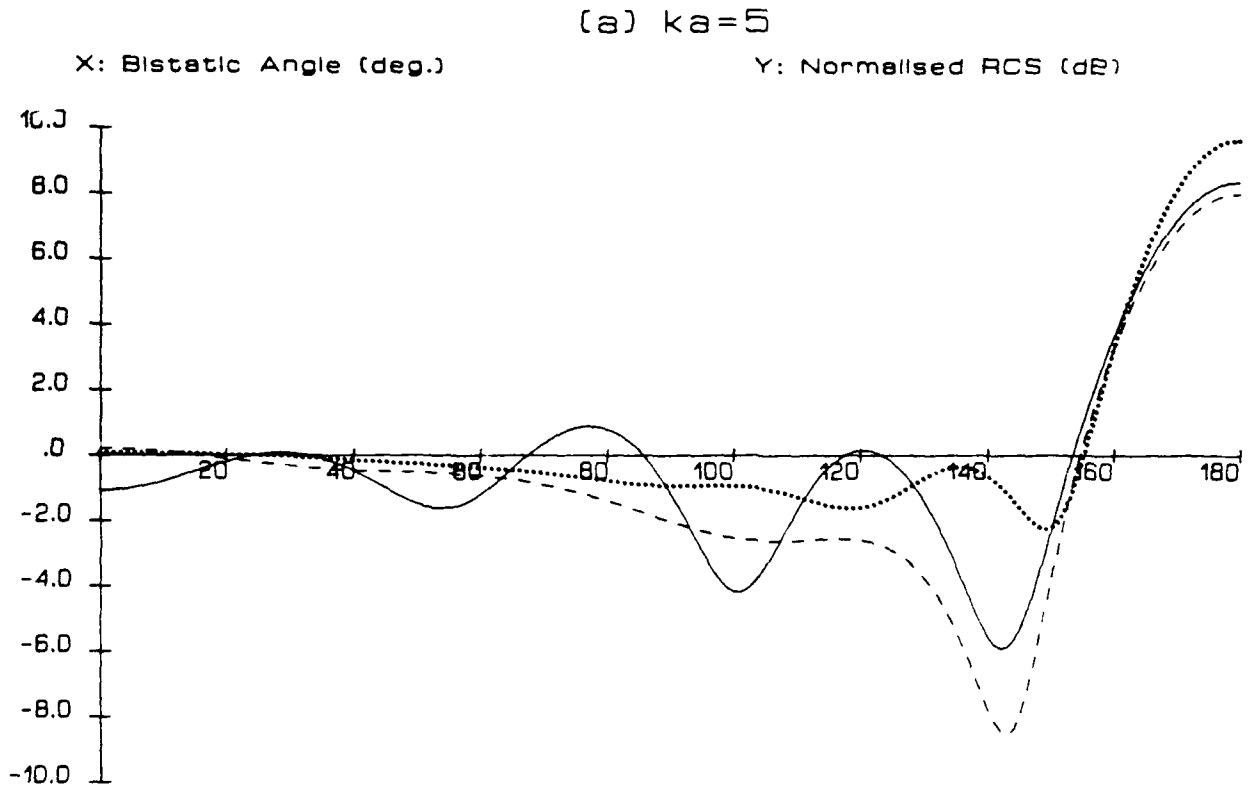

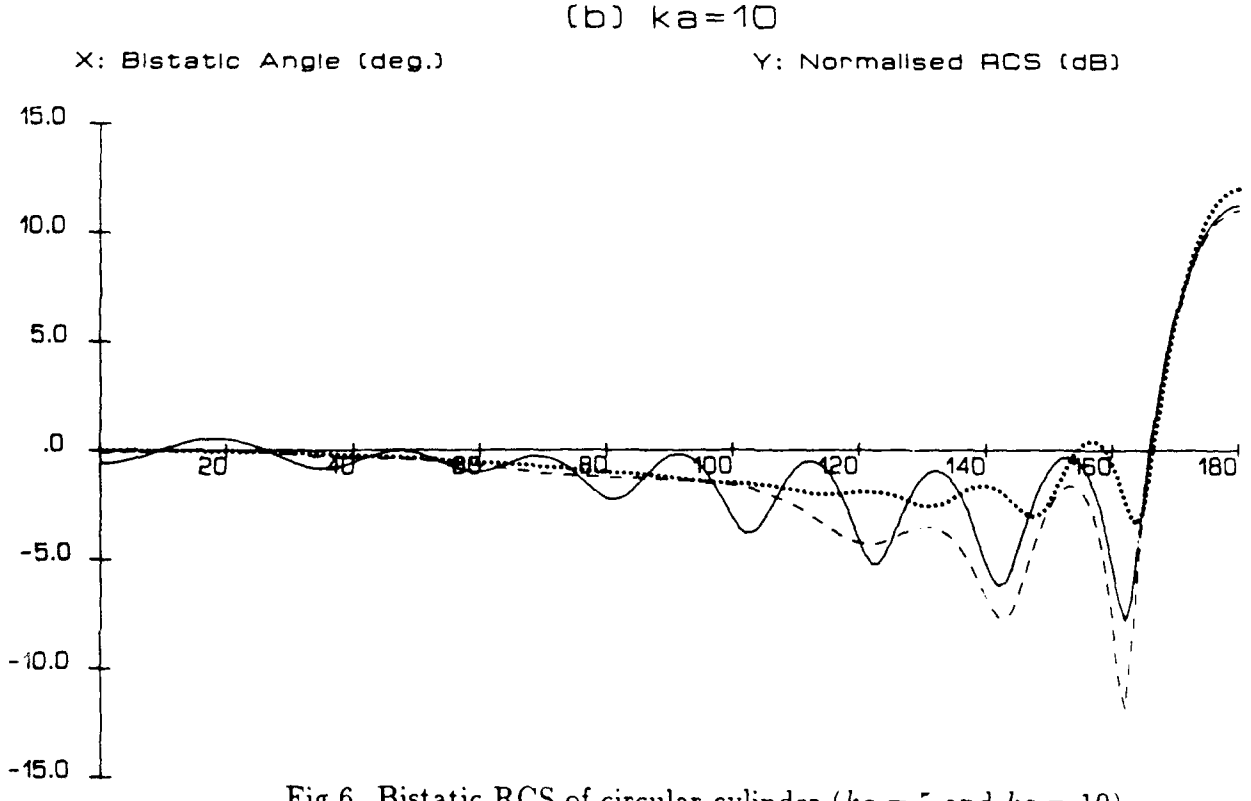

Fig.6. Bistatic RCS of circular cylinder ($ka = $ and $ka = 10$).

—— ADBO solution (using L_r)

..... Exact solution

- - - - PO solution

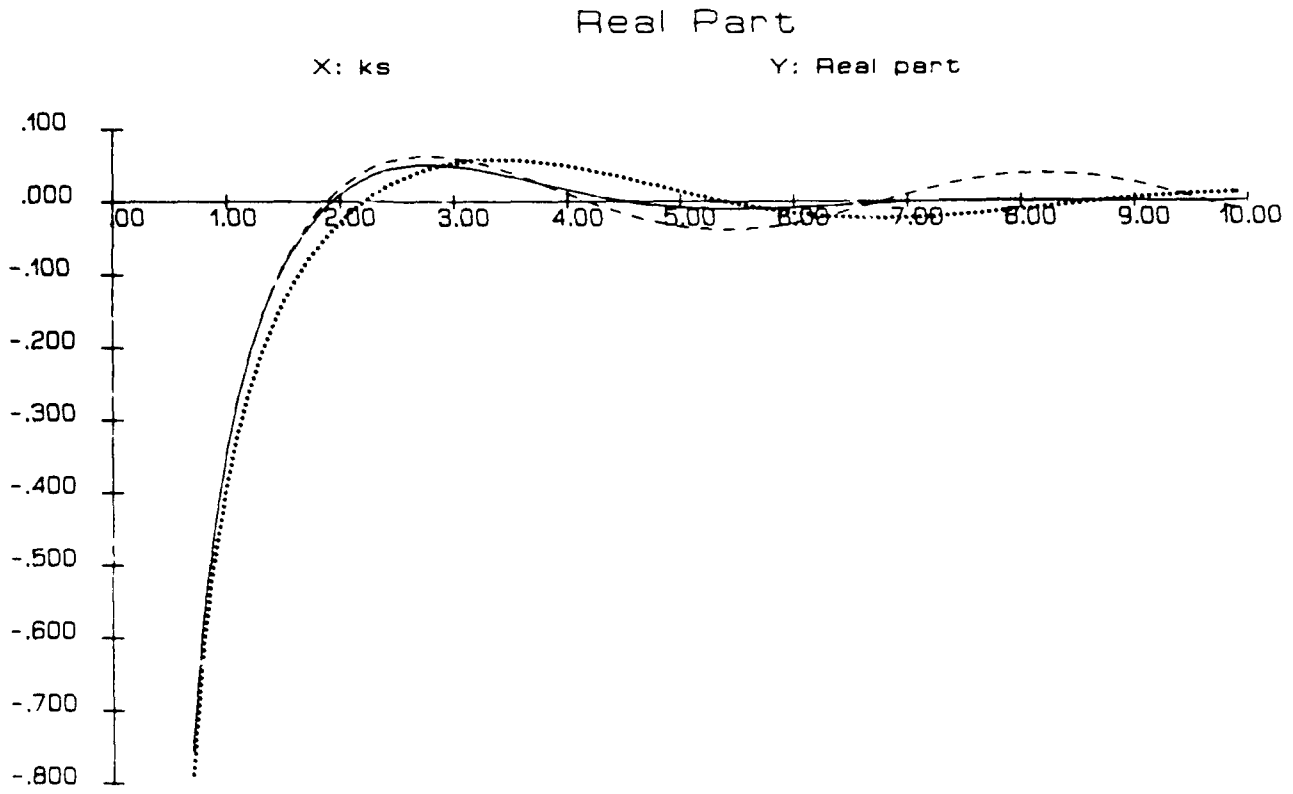

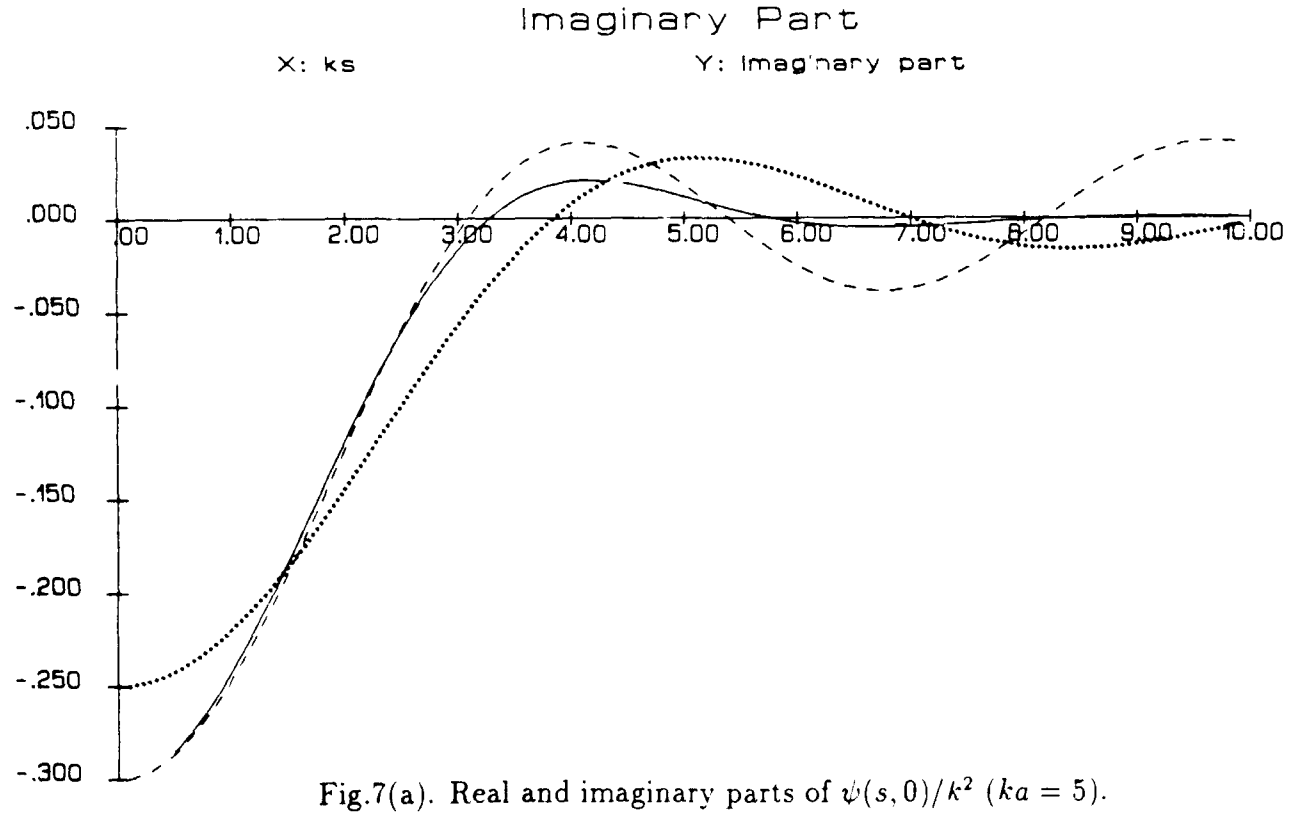

Fig.7(a). Real and imaginary parts of $\psi(s,0)/k^2$ $(ka = 5)$.

—— $\psi^c(s,0)$

..... $\psi^p(s,0)$

- - - - approximation to $\psi^c(s,0)$ (eq.(57))

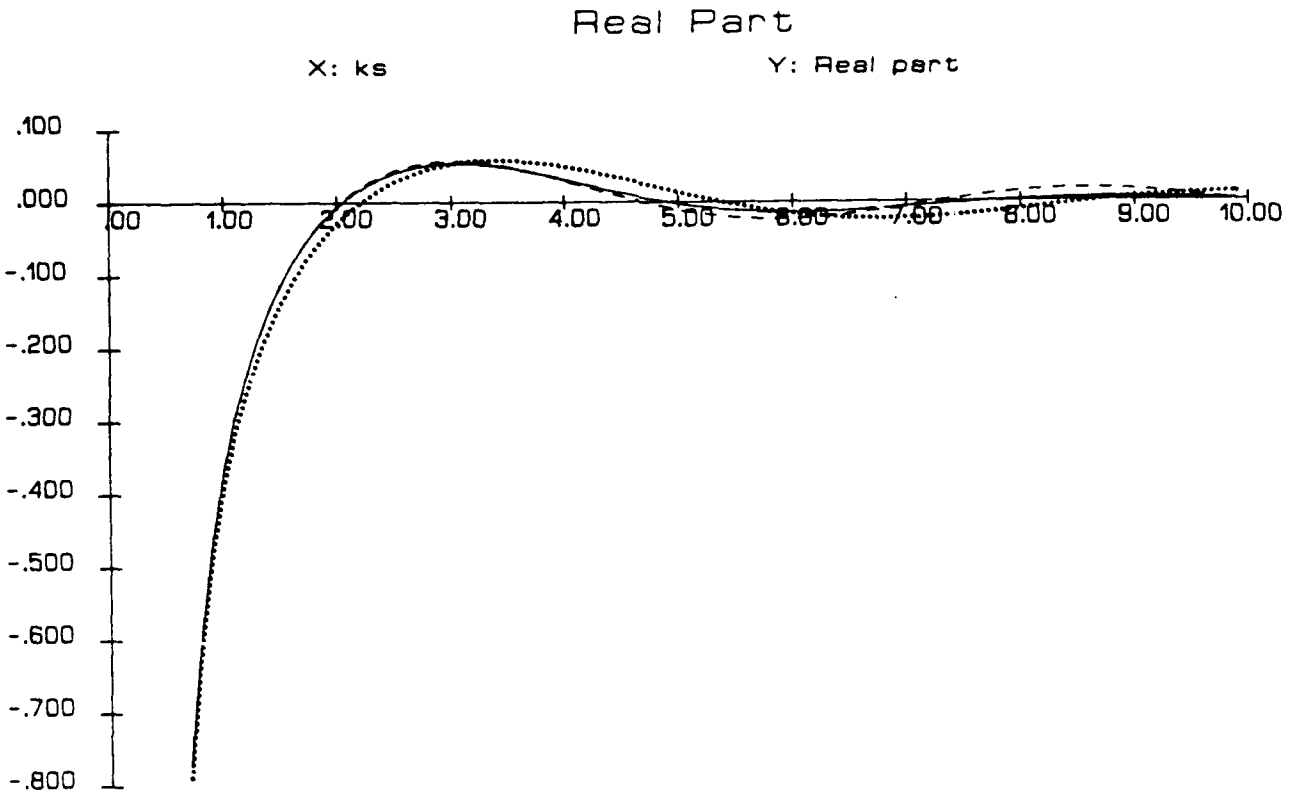

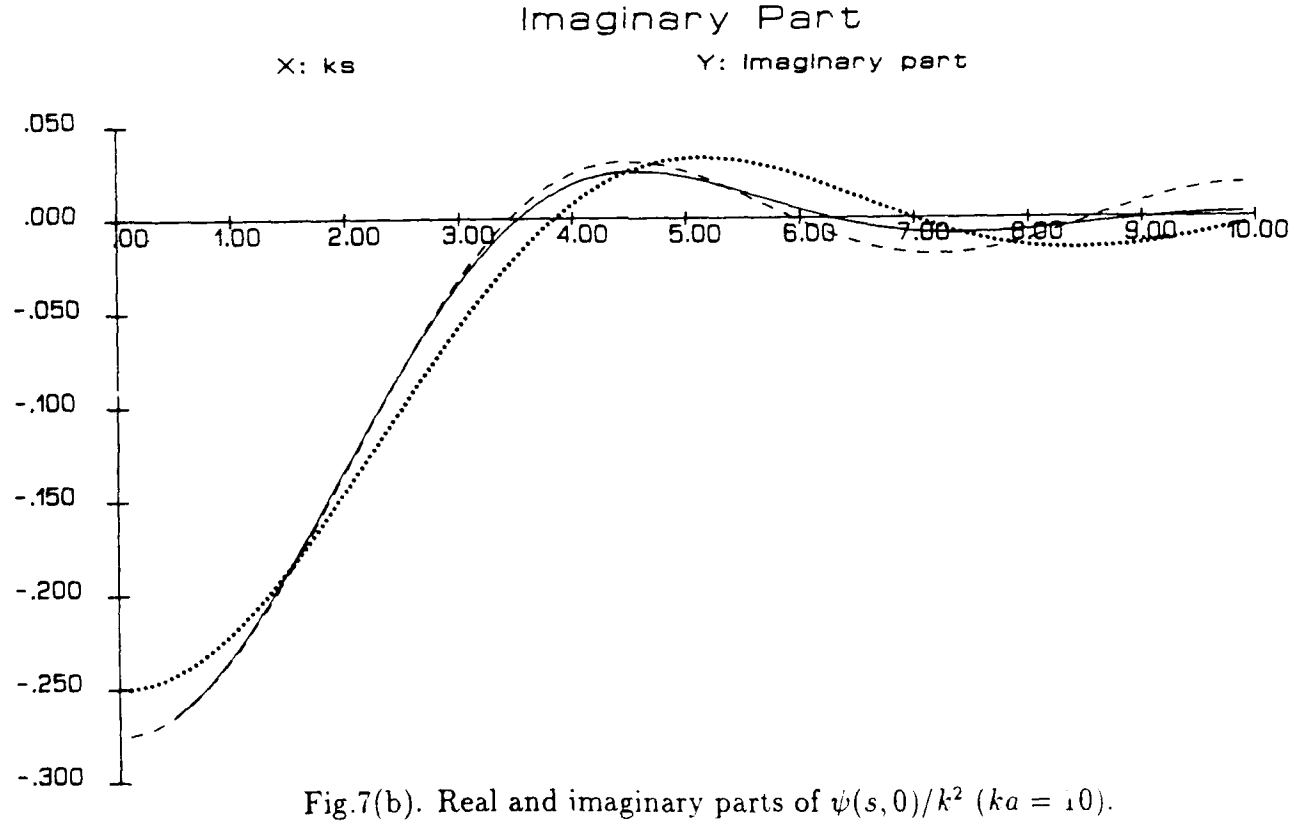

Fig.7(b). Real and imaginary parts of $\psi(s,0)/k^2$ ($ka = 10$).

—— $\psi^c(s,0)$

..... $\psi^p(s,0)$

- - - - approximation to $\psi^c(s,0)$ (eq.(57))

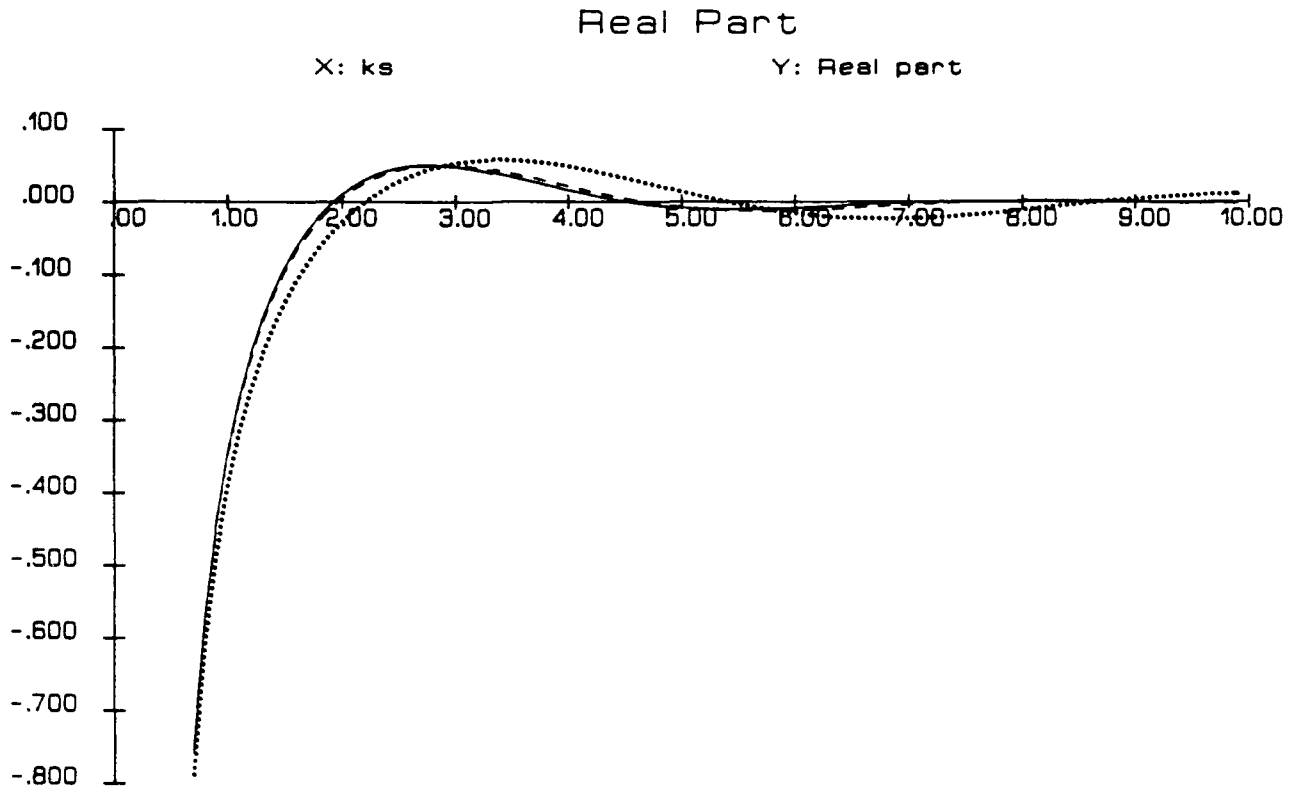

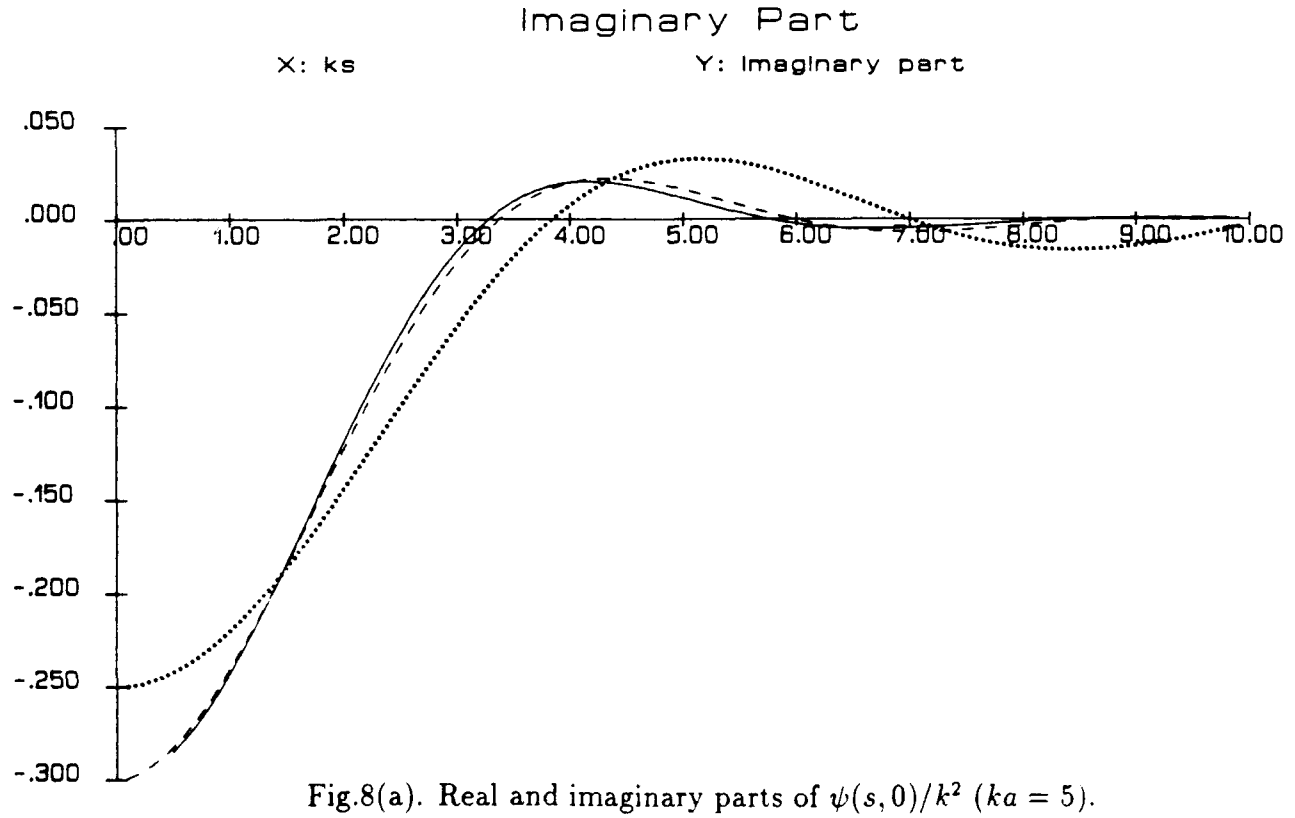

Fig.8(a). Real and imaginary parts of $\psi(s,0)/k^2$ ($ka = 5$).

—— $\psi^c(s,0)$

..... $\psi^p(s,0)$

- - - - approximation to $\psi^c(s,0)$ (eq.(65))

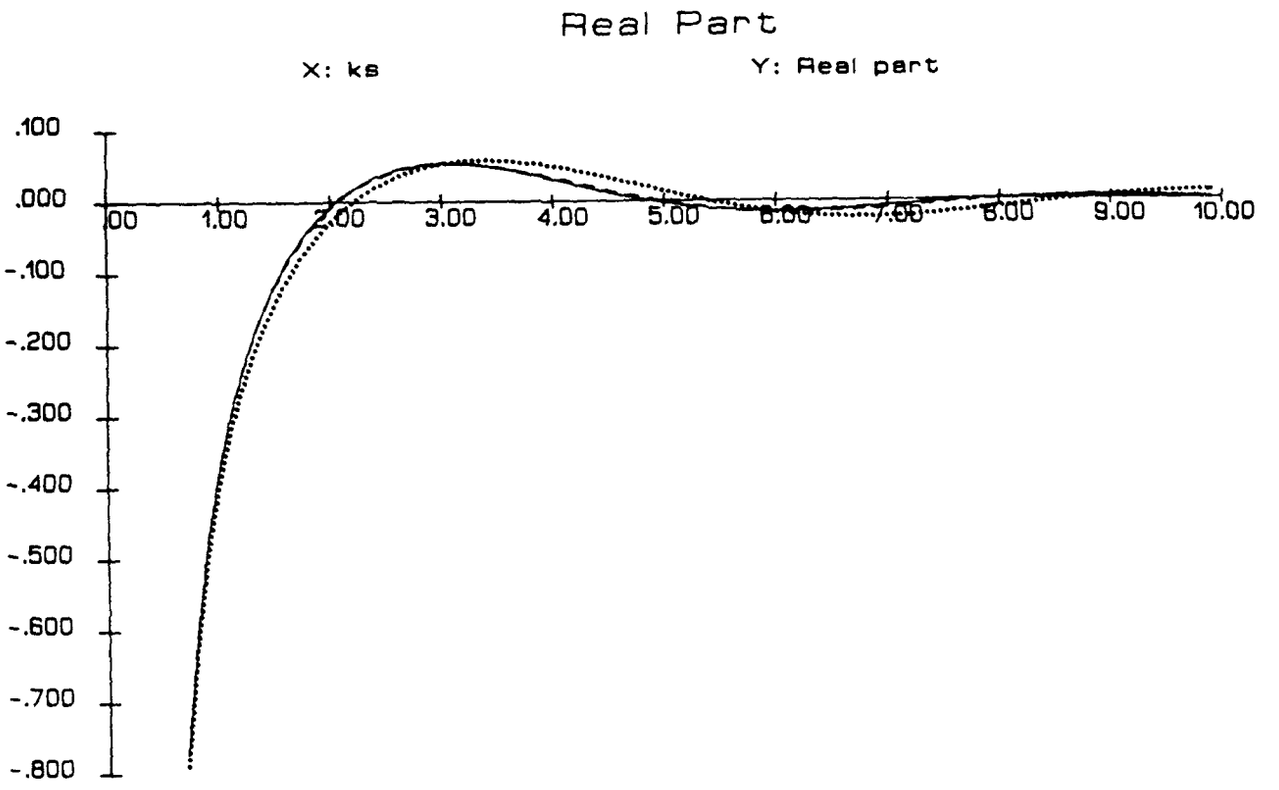

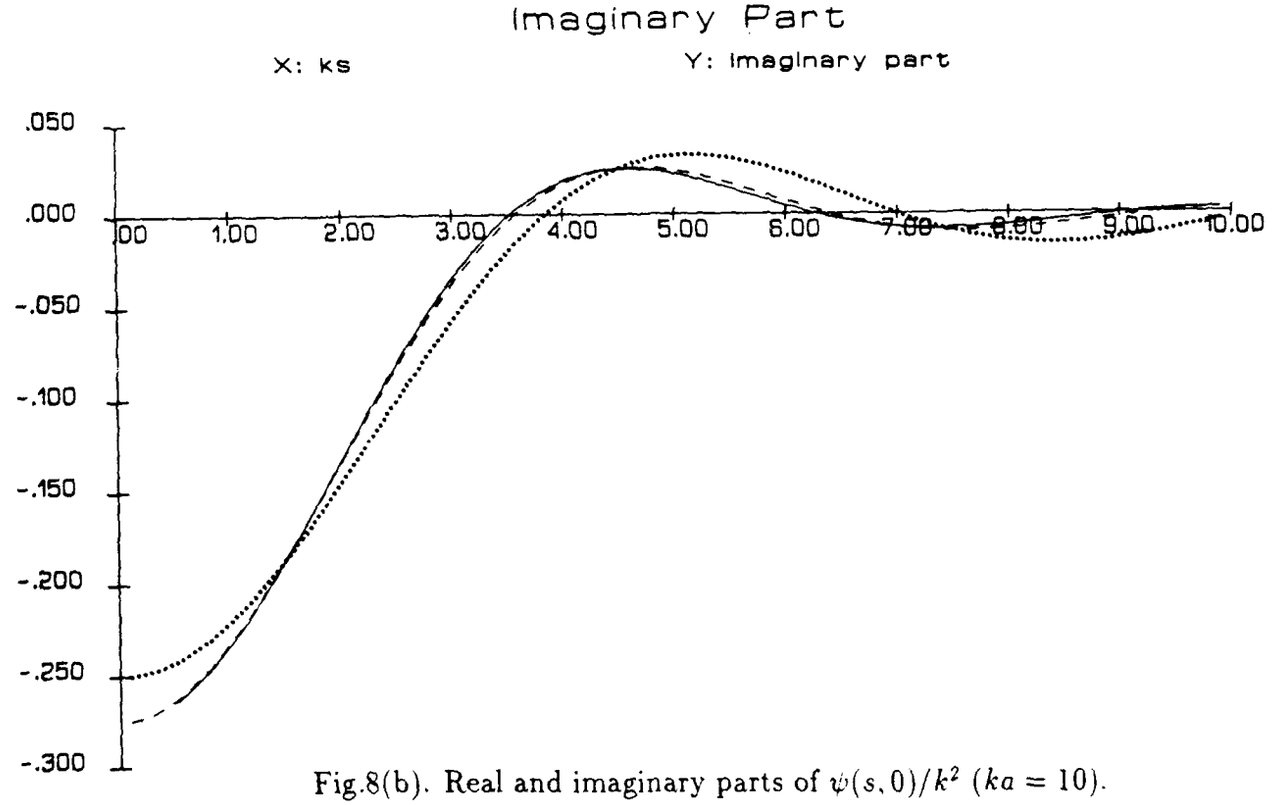

Fig.8(b). Real and imaginary parts of $\psi(s,0)/k^2$ $(ka = 10)$.

—— $\psi^c(s,0)$

..... $\psi^p(s,0)$

- - - - approximation to $\psi^c(s,0)$ (eq.(65))

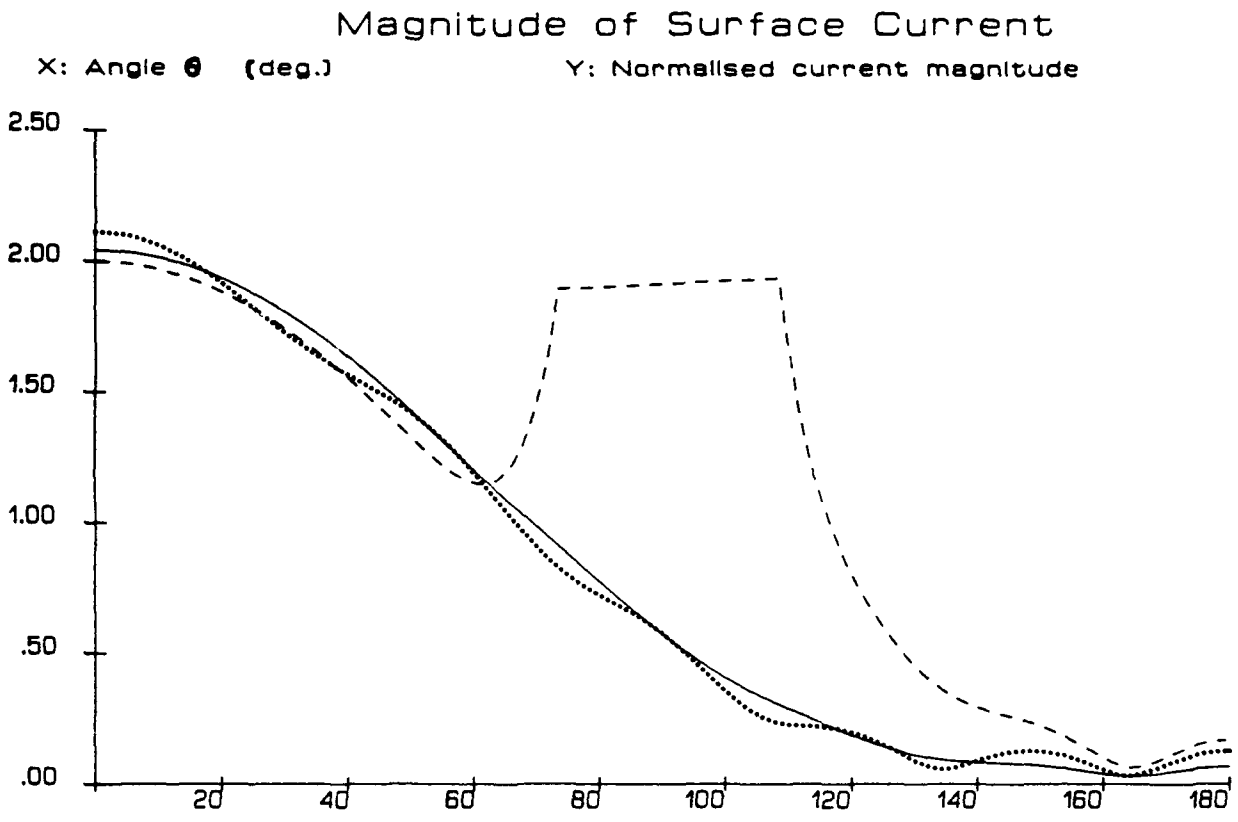

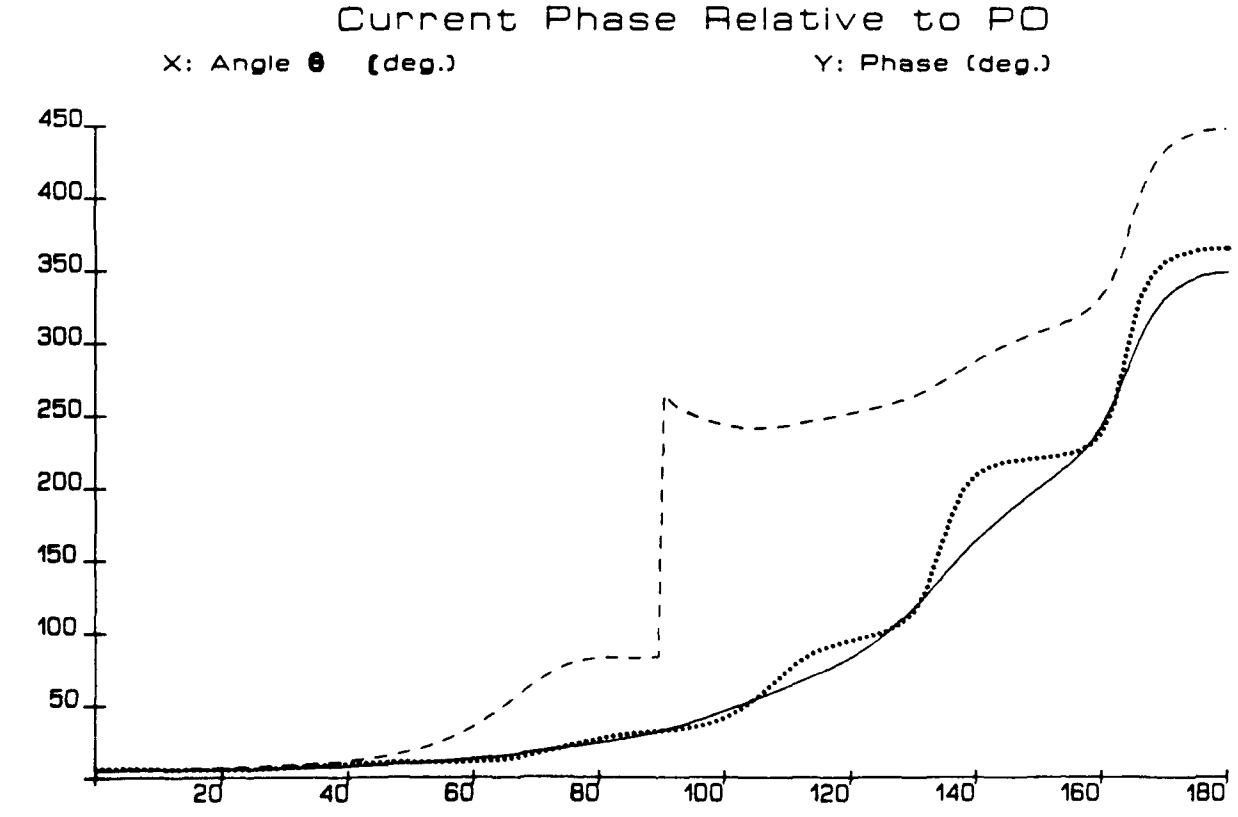

Fig.9(a). IDBO predictions of circular cylinder current ($ka = 5$).

—— using I_π and M_π (eq.(67))

..... using I_∞ and M_∞ (eq.(73))

- - - - using analytic approximation to I_π and M_π (eq.(72))

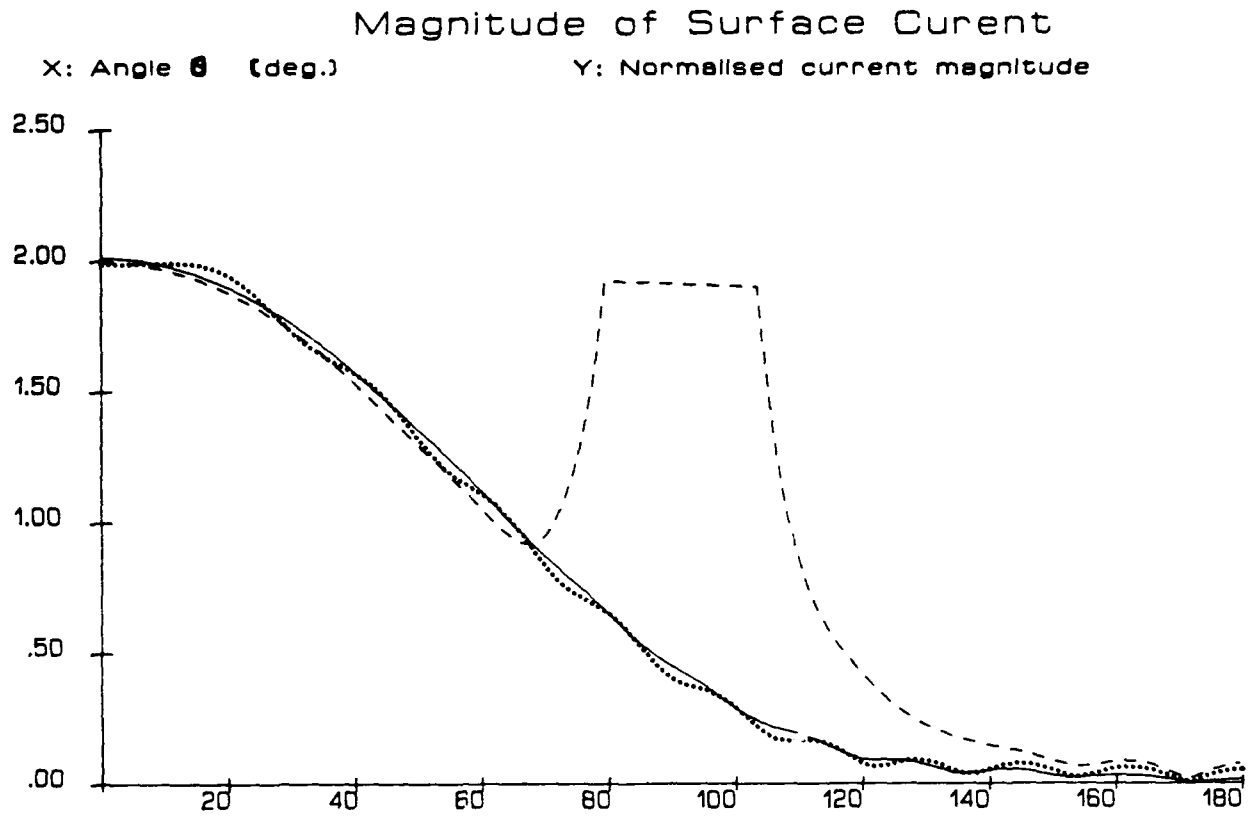

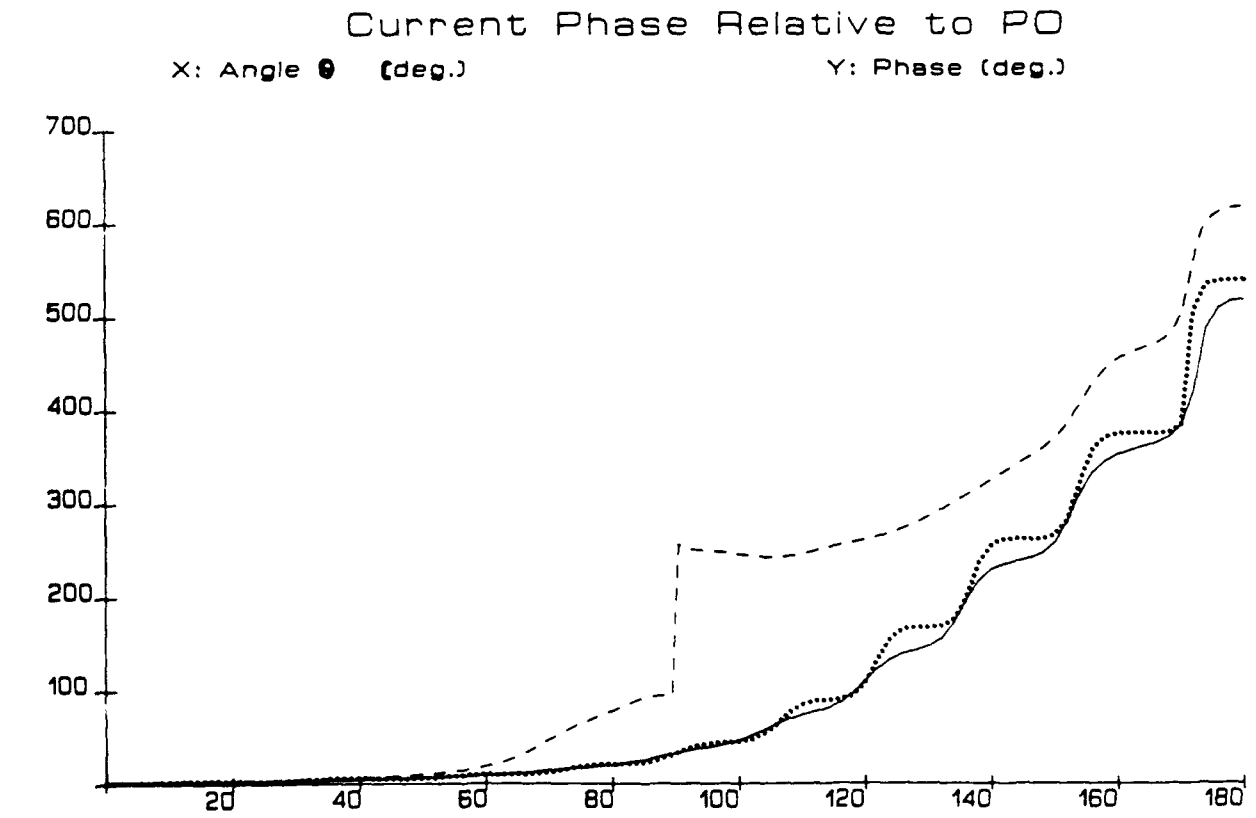

Fig.9(b). IDBO predictions of circular cylinder current ($ka = 10$).

—— using I_π and M_π (eq.(67))

····· using I_∞ and M_∞ (eq.(73))

- - - - using analytic approximation to I_π and M_π (eq.(72))

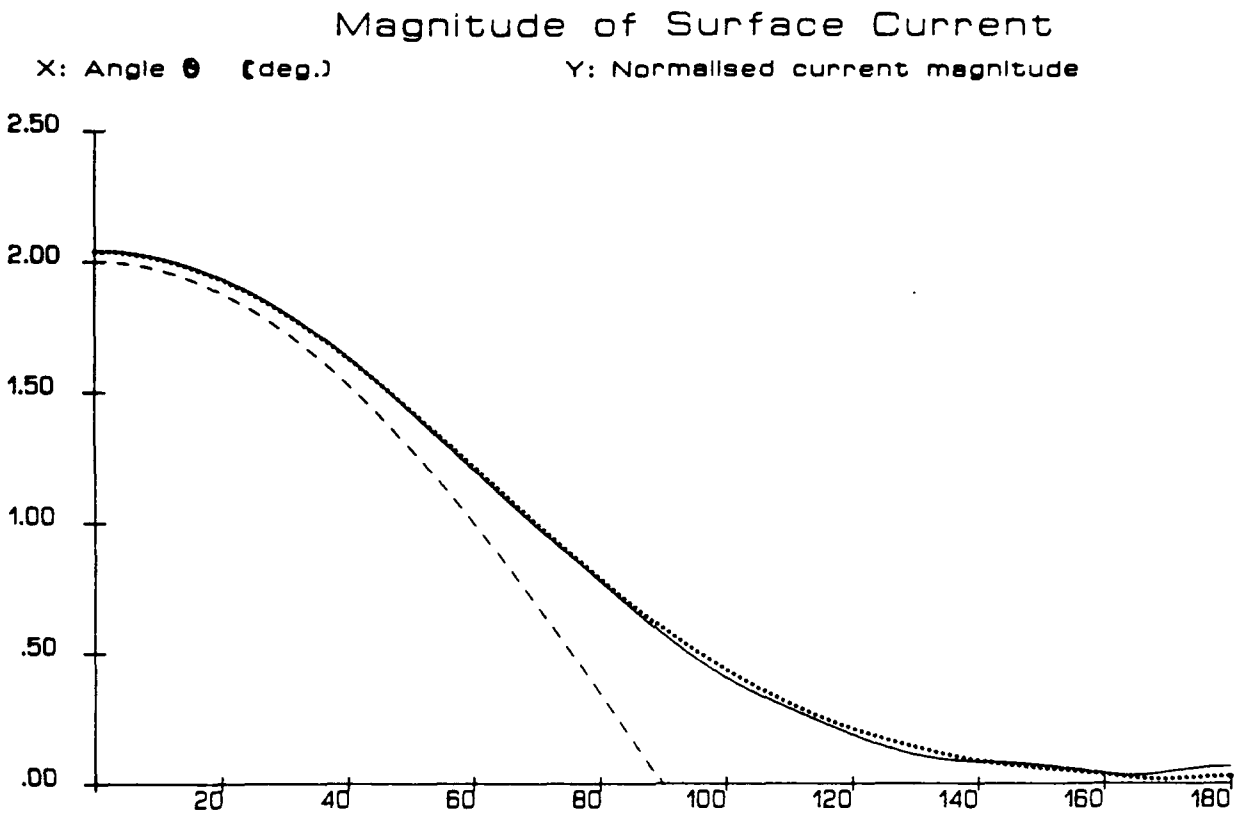

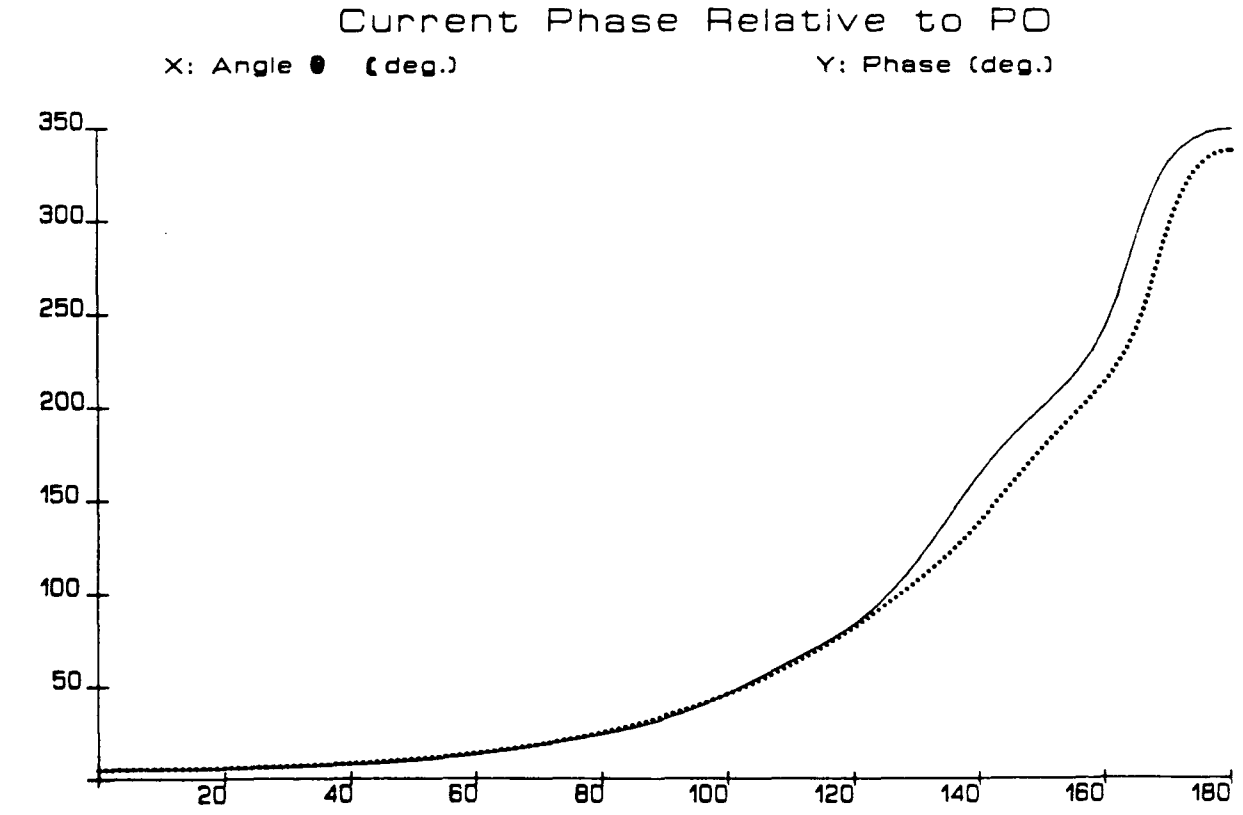

Fig.10(a). Circular cylinder surface current ($ka = 5$).

—— IDBO solution (using I_π and M_π)

..... Exact solution

- - - - PO solution

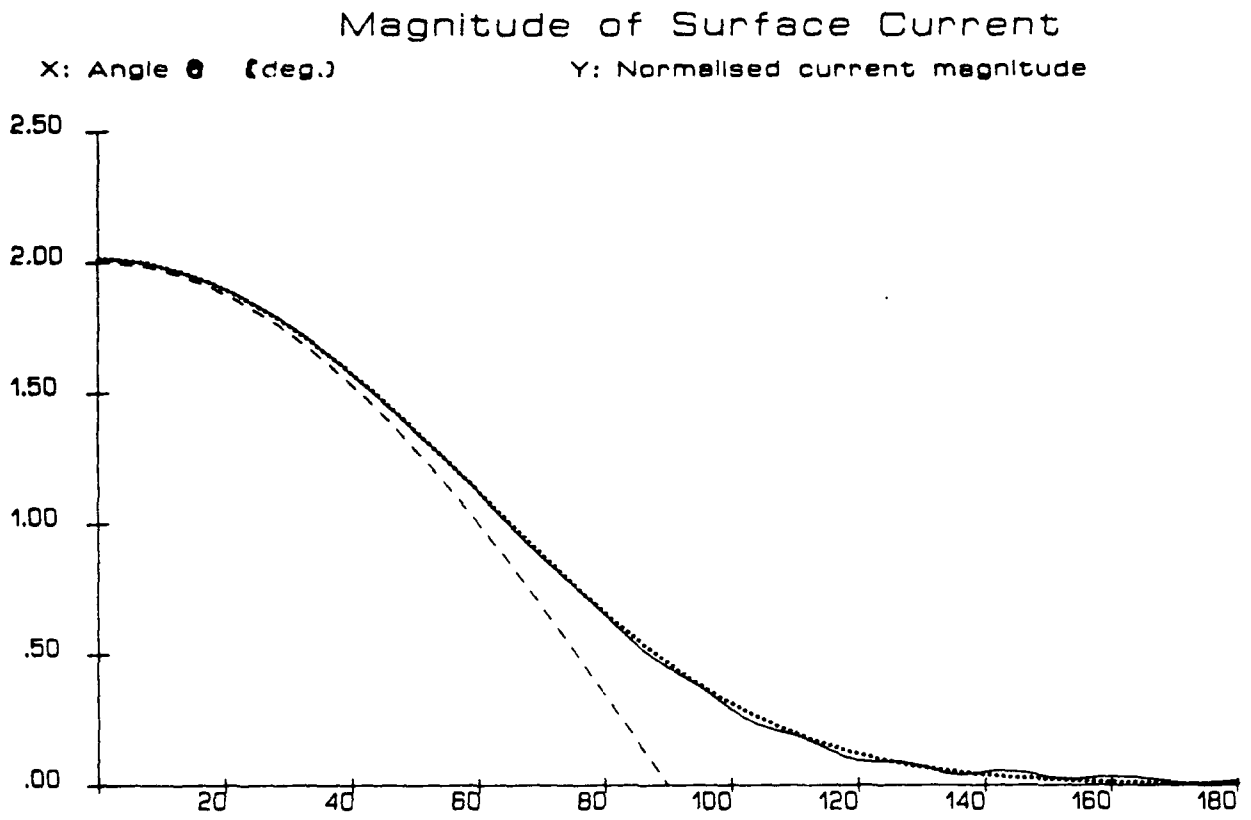

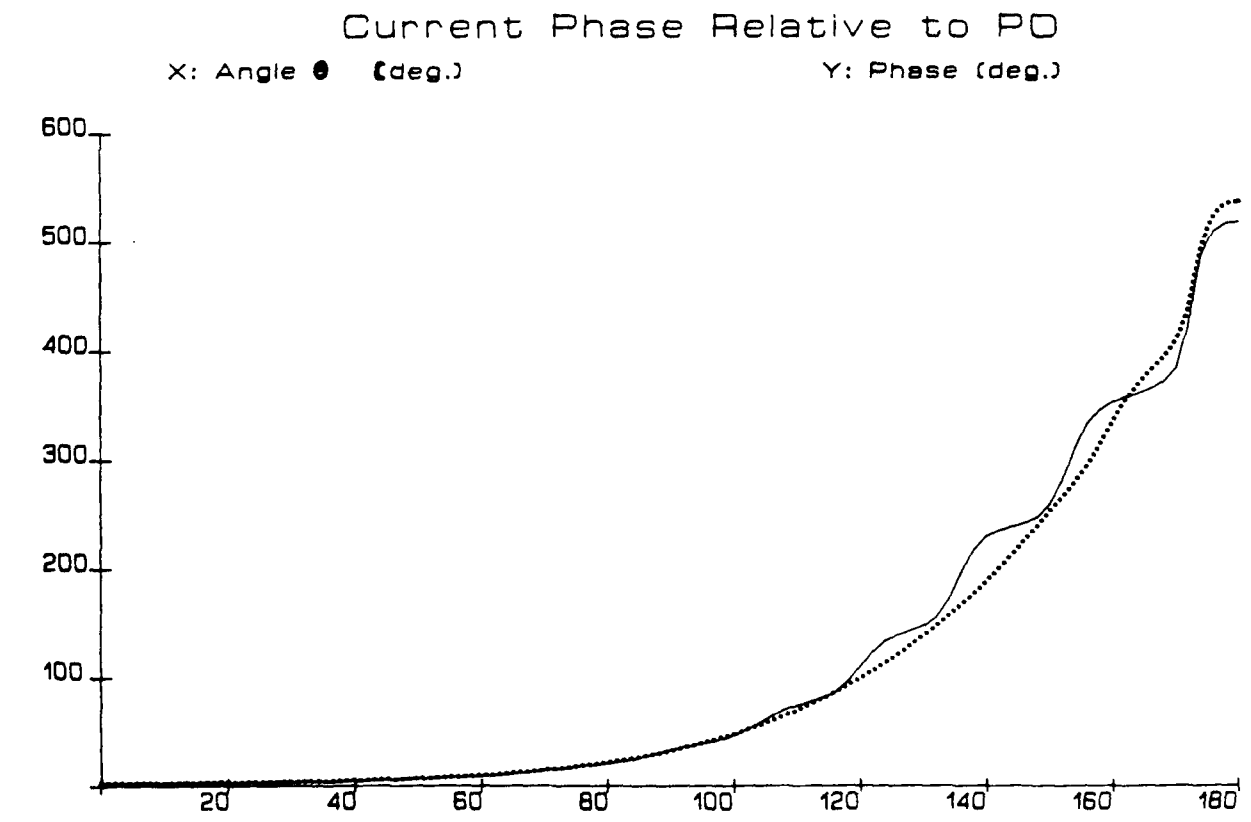

Fig.10(b). Circular cylinder surface current ($ka = 10$).

—— IDBO solution (using I_π and M_π)

..... Exact solution

- - - - PO solution

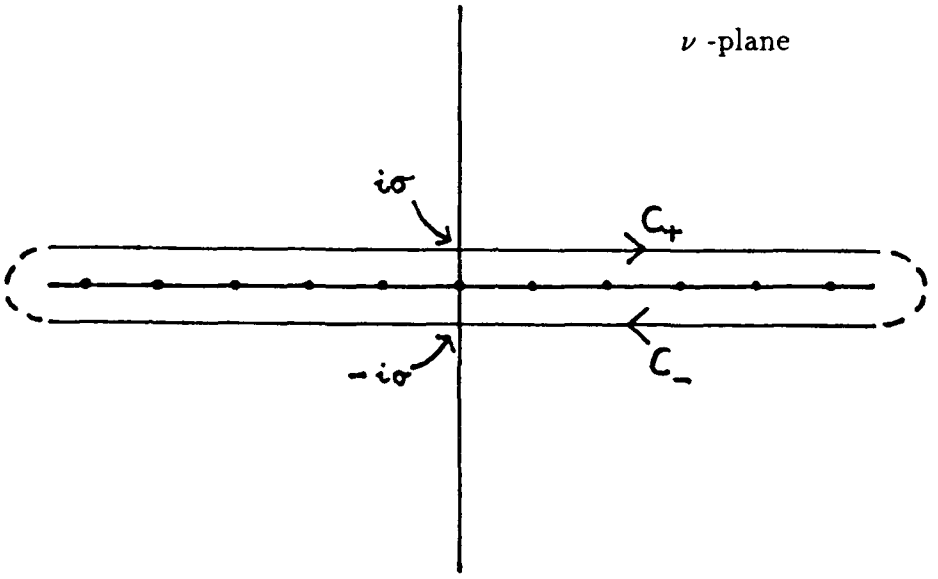

Fig.11. Integration contour for Watson transformation.

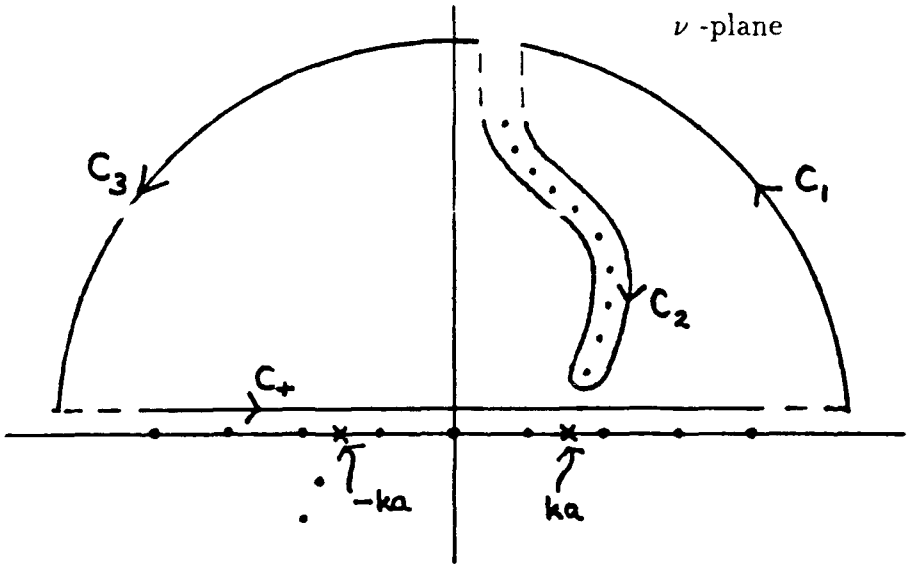

Fig.12. Integration contour C of Eq.(140).

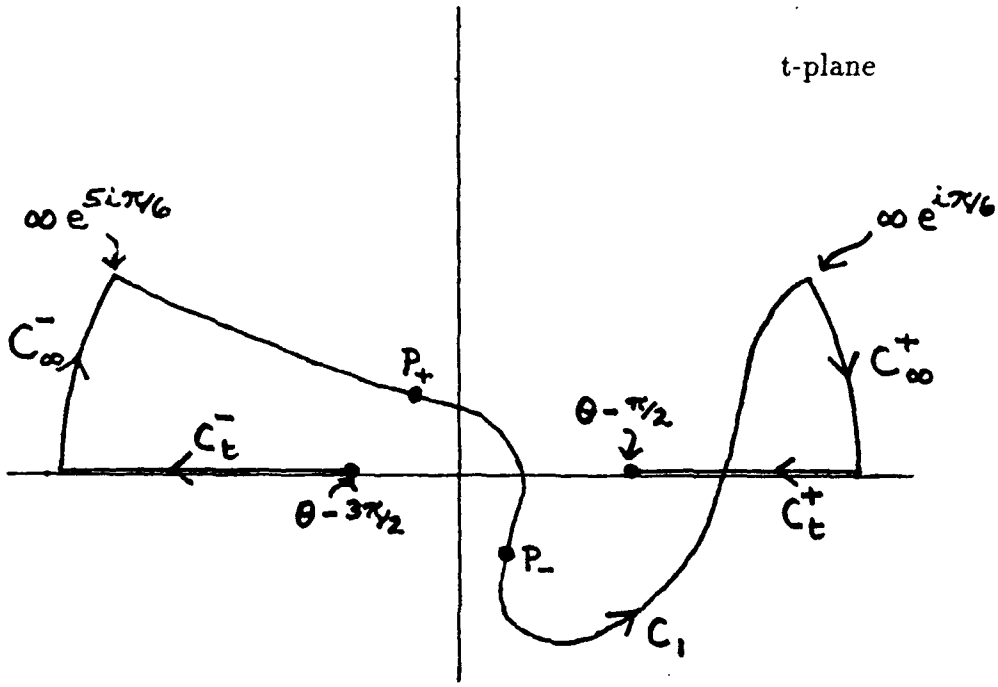

Fig.13. Integration contour C of Eq.(164).

INTENTIONALLY BLANK

REPORT DOCUMENTATION PAGE

DRIC Reference Number (if known) .....

Overall security classification of sheet .....UNCLASSIFIED.....

(As far as possible this sheet should contain only unclassified information. If it is necessary to enter classified information, the field concerned must be marked to indicate the classification eg (R), (C) or (S).

Originators Reference/Report No.	Month	Year
MEMO 4502	JULY	1991

Originators Name and Location
RSRE, St Andrews Road
Malvern, Worcs WR14 3PS

Monitoring Agency Name and Location

Title
ELECTROMAGNETIC SCATTERING BY THE DELTA BOUNDARY OPERATOR METHOD

Report Security Classification	Title Classification (U, R, C or S)
UNCLASSIFIED	U

Foreign Language Title (in the case of translations)

Conference Details

Agency Reference	Contract Number and Period

Project Number	Other References

Authors	Pagination and Ref
KING, I D	57

Abstract

An alternative and rigorous formulation of electromagnetic scattering - the Delta Boundary Operator (DBO) technique - has been reported in the literature. Use of a simple approximation allows fast and accurate calculations of scattering by rough planar surfaces. Here an investigation of the wider applicability of approximate DBO techniques is pursued. Attention is focussed on scattering by simple smooth bodies in the so-called resonance region, where the approximations of high frequency asymptotic techniques are often inadequate. It is shown that application of approximate DBO methods leads to predictions of non-vanishing surface currents in unlit regions and smooth transition currents at shadow boundaries.

Abstract Classification (U,R,C or S)
U

Descriptors

Distribution Statement (Enter any limitations on the distribution of the document)
UNLIMITED